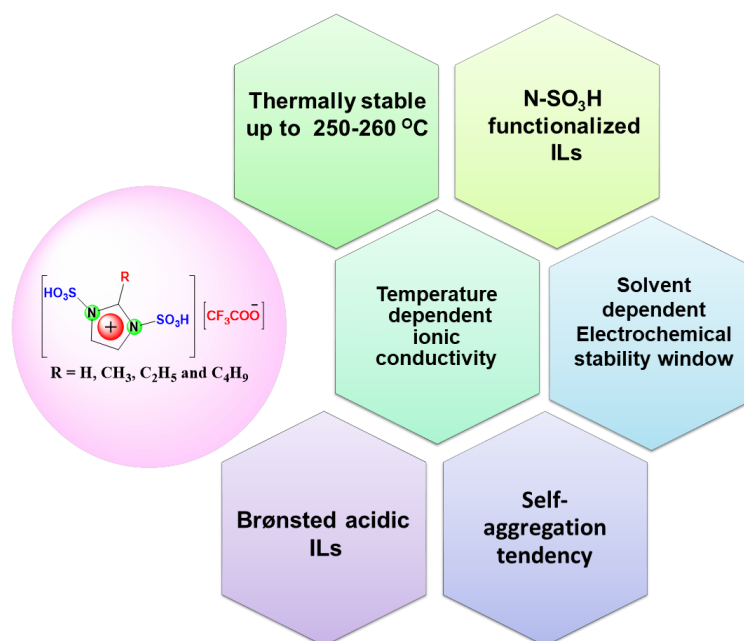# *Chapter 3*

Investigation of the Physical and Electrochemical Behaviour of Direct N-SO₃H Functionalized 1, 3-Disulfo-2-Alkyl-Imidazolium Trifluoroacetate Ionic Liquids in Molecular Solvents

Thermally stable up to 250-260 °C

N-SO₃H functionalized ILs

Temperature dependent ionic conductivity

Solvent dependent Electrochemical stability window

Brønsted acidic ILs

Self-aggregation tendency

HO_3S R SO_3H $[CF_3COO^-]$

R = H, CH₃, C₂H₅ and C₄H₉

3.1 Introduction

The concept of Green Chemistry has become quintessential for encouraging sustainable practices in laboratories and industries. From this perspective, the ionic liquids (ILs) have emerged as a promising environmental friendly alternative to the volatile organic solvents. The ILs have over the years gained prominence in numerous fields like catalysis [1,2], energy conversion devices and fuel cells [3], biomass conversion [4,5], polymer chemistry [6], nanotechnology [7, 8], analytical chemistry [9], sensors [10] etc. Functionalization of these ILs with acidic $-SO_3H$ group has led to development of task-specific ILs (TSILs) which can act as a dual solvent cum catalyst in several organic syntheses [1, 11-13]. Exploration of the unique physicochemical properties of these TSILs has been considered as one of the relevant fields of research in material sciences. The ability to mix and match the cationic and anionic constituents of ILs and functionalize their side chains allows amazing tunability of their physicochemical properties like ionic conductivity, viscosity, thermal stability, moisture sensitivity, electrochemical stability, solubility of diverse solutes in them, and miscibility/immiscibility with a wide range of solvents [14]. Thus, an appropriate combination of the cation-anion pair can generate TSILs with desired characteristics. Over the years, several research articles devoted to the synthesis, physicochemical properties and applications of TSILs have been published [15-21] including $-SO_3H$ functionalized ionic liquids.

The initial studies on the $-SO_3H$ functionalized ionic liquids were carried out by Zolfigol and his group [22-24]. They first synthesized imidazolium-based direct $N-SO_3H$ functionalized ILs and investigated their applications in catalysis. Akbari et al. and Kore et al. also investigated the catalytic activities of $-SO_3H$ functionalized ILs [25, 26]. Then onwards, these investigations of $N-SO_3H$ functionalized ionic liquid materials have been extended to the ammonium, pyridinium and phosphonium cations [27-30]. Later on, Sarma et al. in 2017 reviewed the catalytic uses of all the classes of sulfonic acid tethered Brønsted acidic ILs in organic reactions [31].

The study of physicochemical properties of TSILs is important to identify their proper applications in specific fields including electrochemistry, catalysis, fuel cells and battery, separation medium, biomass conversion etc. For example, the electrochemical uses of the ILs are mostly dependent on their electrochemical windows (EWs), viscosity,

conductivity, melting point, density and thermal stability. The presence of large number of charge-carriers in ionic liquids provides a broad scope to explore them as potential electrolytes for energy conversion devices like batteries and fuel cells. Nonetheless, the higher viscosities and moderate conductivities of the ILs limit such applications. Designing of less-viscous ILs with high ESWs and conductivities is still a challenge. To overcome these challenges and expand the electrochemical uses of the ILs, they are often mixed with various molecular solvents, which can significantly affect their above-mentioned physicochemical properties including viscosities, conductivities, and self-aggregation tendencies through different solvent-ion interactions [32-36].

A significant number of research articles have been published on the physicochemical properties of the existing imidazolium room temperature ionic liquids (RTILs) in their pure state and also their mixtures with co-solvents [32-38]. To enable the practical uses of binary mixtures of IL-molecular solvent in electrochemistry, the study of their ionicity is considered to be indispensable. Boruń et al. measured the conductance of aqueous solutions of 1-alkyl-3-methyl imidazolium tetrafluoroborates as a function of temperature (283.15 to 318.15 K) and observed the complete dissociation of these ILs in water [21]. Thawarkar et al. investigated the effect of molecular solvents on the molar conductivity of protic ionic liquids (PILs). The molar conductivities were measured for binary mixtures of three PILs i.e. [HmIm][HCOO], [HmIm][CH$_3$COO], and [HmIm][CH$_3$CH$_2$COO] in six molecular solvents such as water, methanol, ethanol, dimethyl sulfoxide, nitrobenzene and acetonitrile at 298.15 K [39]. The Kamlet-Taft solvatochromic parameters (E^T_N, α, and β) of the solvents were used as their polarity indicators. The conductivity values for all PILs increases with increasing polarity of the molecular solvent [39]. The same group later employed conductometry and NMR studies to observe the ionicities of the binary mixtures of nine protic and aprotic ionic liquids in three molecular solvents namely water, dimethyl sulfoxide and ethylene glycol within the temperature range of 293.15–323.15 K [32]. They observed greater ionicities of the aprotic imidazolium ILs compared to those of the protic imidazolium ILs [32]. In these solvents, the conductivity of ILs expressed a typical temperature dependent Arrhenius behaviour. Pereiro et al. investigated ways to generate high ionicity by adding inorganic salts to pure ionic liquids [40]. Rupp et al. studied the ionicities of imidazolium and ammonium based ionic liquids as function of their sizes [41].

Buchner and co-workers investigated the ion associative behaviour of 1-butyl-3-methylimidazolium chloride [bmin][Cl] in acetonitrile and water by employing dielectric spectroscopy technique [42]. Dorbritz et al. utilized mass spectrometry to evaluate the aggregate forming tendencies of the aprotic imidazolium ionic liquids in different molecular solvents [20]. The sizes of the aggregates were found to decrease with the increasing solvent polarity and decreasing ionic liquid concentration.

The presence of solvents is known to affect the electrochemical stability of ionic liquids. O'Mahony et al. showed that the electrochemical stability windows (ESWs) of a large number of 1-alkyl-3-methyl-imidazolium based RTILs containing $[BF_4]^-$ and $[PF_6]^-$ anions were narrowed due to the presence of water as an impurity [43]. This was accounted for undesirable evolution of HF via hydrolysis of these anions. Further, the nature of constituent ions also affects the electrochemical stability of the ILs. In general, the ammonium based ILs are known to express larger electrochemical stability windows (ESWs) compared to imidazolium based ILs [14]. Zhou et al. examined the electrochemical stability and ionic conductivities of the imidazolium-based mono-ether functional ionic liquids and correlated the results with the cation and anion structures [44].

Thus, over the years several studies on the imidazolium based ionic liquids were conducted. However, a detailed investigation of the physicochemical properties of N-SO_3H functionalized ionic liquids was not conducted before. In our present work, we carried out a detailed investigation on the effects of C-2 alkyl substituent of 2-alkyl (or H)-1, 3-disulfoimidazolium trifluorocetate [RSIM][TFA] ionic liquids (where R = H, CH_3, C_2H_5 and n-C_4H_9) (**Scheme 3.1**) on the values of their ionic conductivity and electrochemical stability window (ESW) in the two molecular solvents MeOH and MeCN. Further, the effects of the C-2 alkyl substituent of these ILs on their density, thermal stability and Brønsted acidity were also evaluated. The Kamlet-Taft solvatochromic parameters of the molecular solvents were used as their polarity indicators and were used to justify the variation of the conductivity values of the ILs in them. The influence of +I inductive effect of the C-2 alkyl groups and the interactions between molecular solvents with the constituent ion-pairs of the ILs, on their ESWs was studied using the cyclic voltammetry (CV) technique.
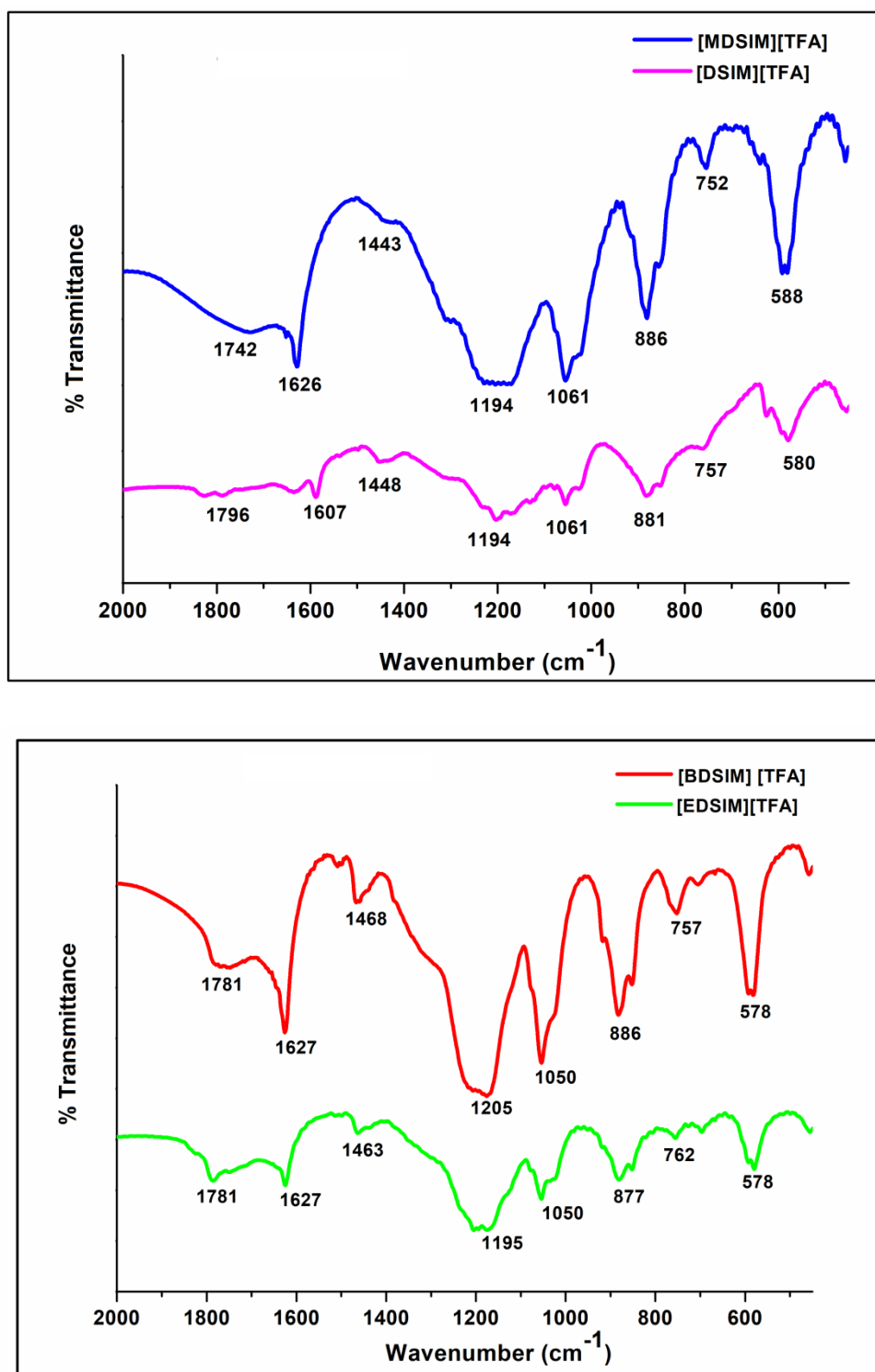
3.2 Results and Discussion

3.2.1 Characterization of the N-SO₃H functionalized Brønsted acidic ionic liquids (BAILs)

The four N-SO$_3$H functionalized BAILs were synthesized according to the standard procedure (**Scheme 3.1**) [1]. The BAILs (**Fig.3.1**) characterized by using analytical techniques like FT-IR, NMR (^{1}H and ^{13}C) and CHN elemental analysis.

Scheme 3.1: Synthesis of the N-SO$_3$H functionalized BAILs.

Fig. 3.1: Structures of the N-SO$_3$H functionalized BAILs.

3.2.1.1 FT-IR analysis

FT-IR spectra of the four N-SO$_3$H functionalized BAILs are displayed in **Fig.3.2** against their respective possible vibrations of different functional groups or bonds in the 500–2000 cm^{-1} region. The FT-IR band assignments of the BAILs are listed in **Table 3.1**.

Fig. 3.2: FT-IR spectra of the BAILs.

Table 3.1: FT-IR band assignments of the BAILs.

Peaks (cm^{-1})	Assignments
572–587	-SO$_3$H (bending)
750–760	out of plane ring bending of -CH bond

870–885	N-S stretching
1040–1060	S-O symmetric stretching
1178–1192	S-O asymmetric stretching
1441–1468	C-H bending of -CH$_3$ group
1640–1620	-C=C- stretching
1730-1790	C=O stretching
2910-2929	C-H stretching
3450-3400	-OH stretching due to intermolecular H-bonding among IL molecules

3.2.1.2 NMR analysis

Two single proton peaks in the ^{1}H NMR spectra of the ILs around 14.3-11.9 ppm confirmed the attachment of two -SO$_3$H groups through nitrogen atom of the imidazolium cation. Other characteristic signals of the imidazolium protons and C-2 alkyl groups were observed in the aromatic and aliphatic regions respectively. Each of the ^{13}C NMR spectrum of the ILs displayed characteristic C=O signal in the range of 155–170 ppm proving the existence of CF$_3$COO$^-$ anion in the ILs. **Section 3.4.3** shows the NMR spectra (^{1}H & ^{13}C) of the ILs [EDSIM][TFA] and [BDSIM][TFA].

3.2.2 Investigation of the physicochemical properties of the BAILs

3.2.2.1 Thermogravimetric analysis (TGA)

Thermogravimetric analysis of the four 1,3-disulfoimidazolium ionic liquids [DSIM][TFA], [MDSIM][TFA], [EDSIM][TFA] and [BDSIM][TFA] revealed their three-step degradation pattern (**Fig.3.3**). The first step of the plots showed an approximate 5-25% release of physisorbed water around 100 °C. The maximum physisorbed water was released in case of [BDSIM][TFA], whereas it was minimum in case of [DSIM][TFA]. This study provides us information about the unusual increase in the hydrophilic properties of these ILs with the increasing carbon chain length of the C-2 alkyl groups of the imidazolium cation. This can be attributed to the combination of two factors. Firstly, the increasing +I inductive effect of the alkyl groups may reduce the positive charge density on the imidazolium cation, for which, we can expect the following descending order of ionic strength among the constituent ion-pairs of the four ILs: [DSIM][TFA] >[MDSIM][TFA] >[EDSIM][TFA] >[BDSIM][TFA].

As a result, there is a strong probability for the maximum water molecules to take part in H-bonding interactions with the CF_3COO^- anion of the weakly bound ion-pair of [BDSIM][TFA] ionic liquid [45]. Secondly, the acidic C-2 position of imidazolium cation will increase the number of H-bonded water molecules for the [MDSIM][TFA] ionic liquid containing three acidic protons of the C-2 methyl group compared to the single C-2 proton of the [DSIM][TFA] ionic liquid [46]. The TGA plots also expressed maximum thermal stabilities of the four ILs up to 250-260 °C with a slight variation based on the sizes of alkyl groups, followed by an another weight loss in the range of 320-350 °C.
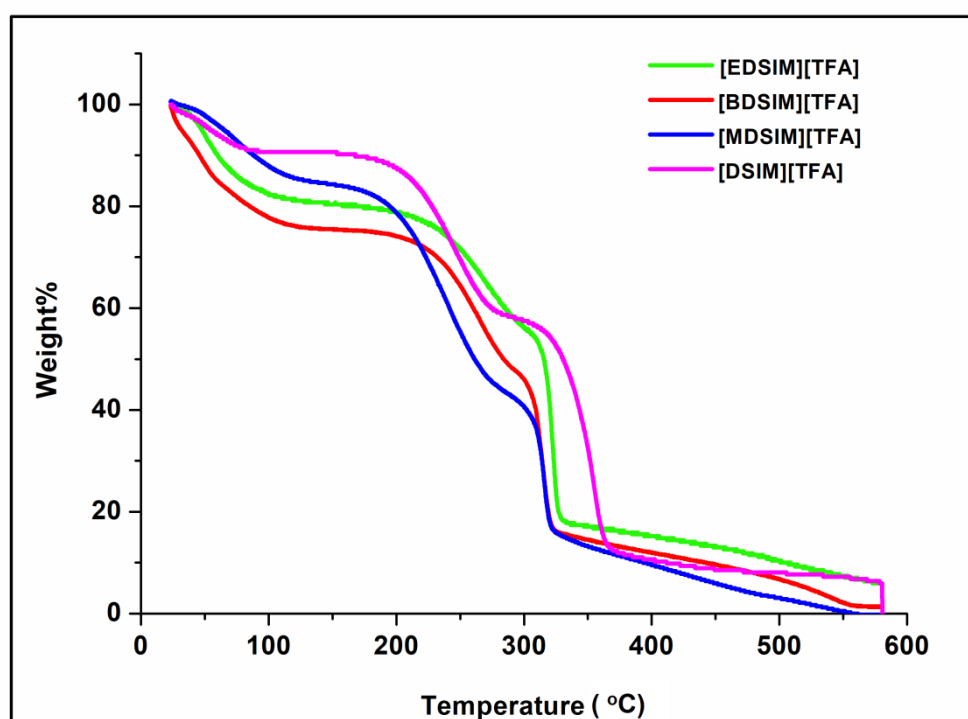
Fig. 3.3: TGA plots of the BAILs.

3.2.2.2 Hammett acidity

The relative Brønsted acidity of the parent chloride based ILs, 2-alkyl-1, 3-disulfoimidazolium chloride [RSIM][Cl] (where R=H, Me, Et & n-Bu) and also counter anion exchanged 2-alkyl-1,3-disulfoimidazolium trifluoroacetate [RSIM][TFA], were determined by comparing the values of Hammett acidity function H^o (**Table 3.2**) obtained from their UV–Vis Hammett plots according to the standard method (**Fig.3.4 A & B**) in ethanol solution [1, 18] using the **Equation 1.4** from **chapter 1**:

$$H^o = pK(IH^+) \text{ (aq)} + \log[I]/[IH^+] \qquad \textbf{(Equation 1.4)}$$

Here pK(I)aq. expresses pKa value of the basic indicator in aqueous solution. The acidity of each series of the IL decreases slowly with the increasing +I effect of the C-2 alkyl substituent of the imidazolium cation. This may be expected as an outcome of the reduction of electron deficient character of the imidazolium cation with the increasing +I effect of the C-2 substituent.

Table 3.2: Hammett acidity functions H^o of the ionic liquids**.**

Entry	IL	A_{max}	[I]%	[HI]%	H^o
1	4-nitroaniline	1.35	100	-	-
2	[BDSIM][Cl]	0.71	52.49	47.51	1.03
3	[EDSIM][Cl]	0.67	49.51	50.49	0.98
4	[MDSIM][Cl]	0.62	45.72	54.27	0.92
5	[DSIM][Cl]	0.52	38.36	61.64	0.78
6	[BDSIM][TFA]	0.59	44.08	55.91	0.89
7	[EDSIM][TFA]	0.48	35.31	64.68	0.73
8	[MDSIM][TFA]	0.45	33.38	66.61	0.69
9	[DSIM][TFA]	0.35	26.02	73.97	0.54
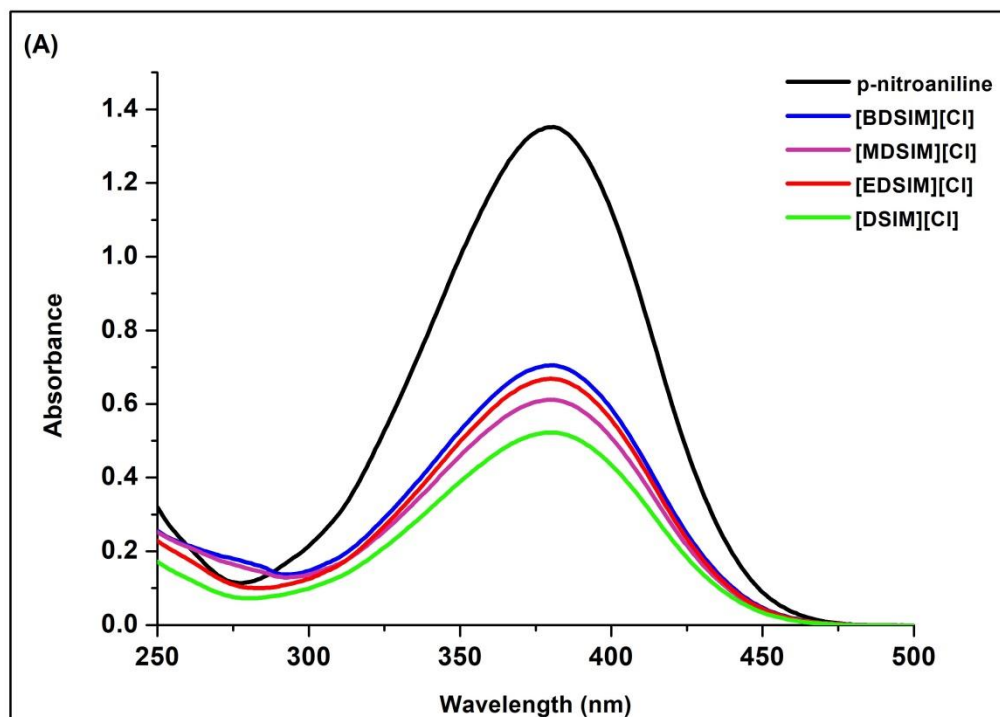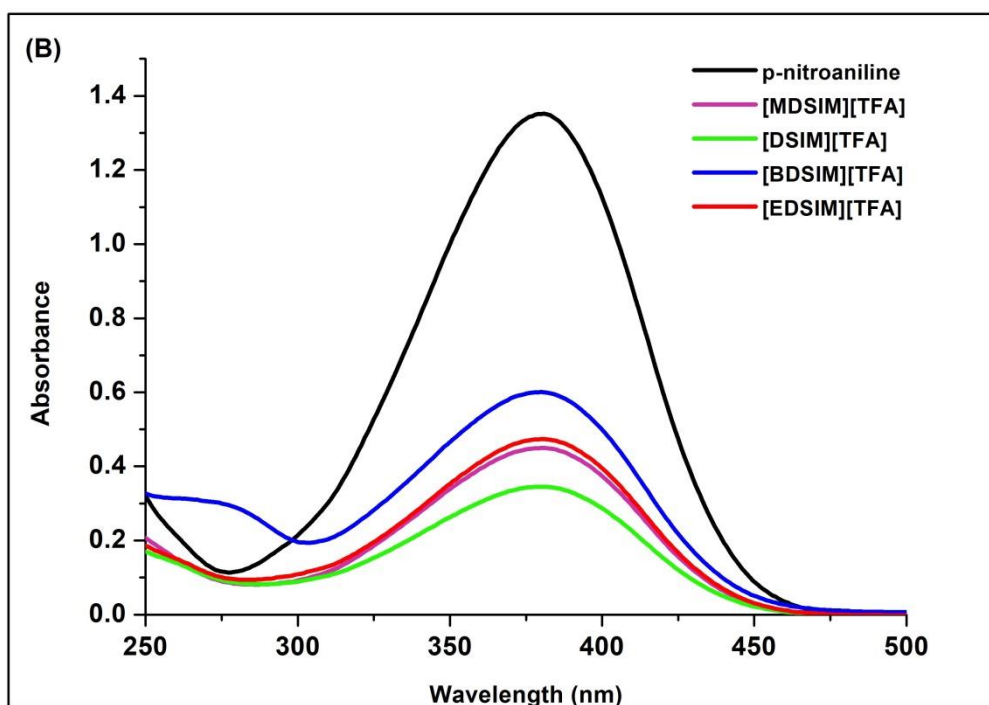
Fig. 3.4: Hammett acidity plots of the (A) Cl based ILs (B) TFA based ILs.

3.2.2.3 Density of the BAILs

Densities of the four N-SO$_3$H [RSIM][TFA] ILs were measured using a pycnometer at 298.15 K. The density values are presented in **Table 3.3**. The plot of density vs number of carbon atoms of the C-2 alkyl groups of the ILs is shown in **Fig. 3.5**. The plot expressed a lowering of the density values of the ILs with the increasing size of the C-2 alkyl groups. This is because, the addition of -CH$_2$ group to the imidazolium ring increases the free space between two IL molecules and thus reduces the compactness of the ILs.

Table 3.3: Density of Ionic Liquids at 298.15 K.

Ionic Liquids	Density (g/mL)
[DSIM][TFA]	1.62
[MDSIM][TFA]	1.59
[EDSIM][TFA]	1.56
[BDSIM][TFA]	1.49
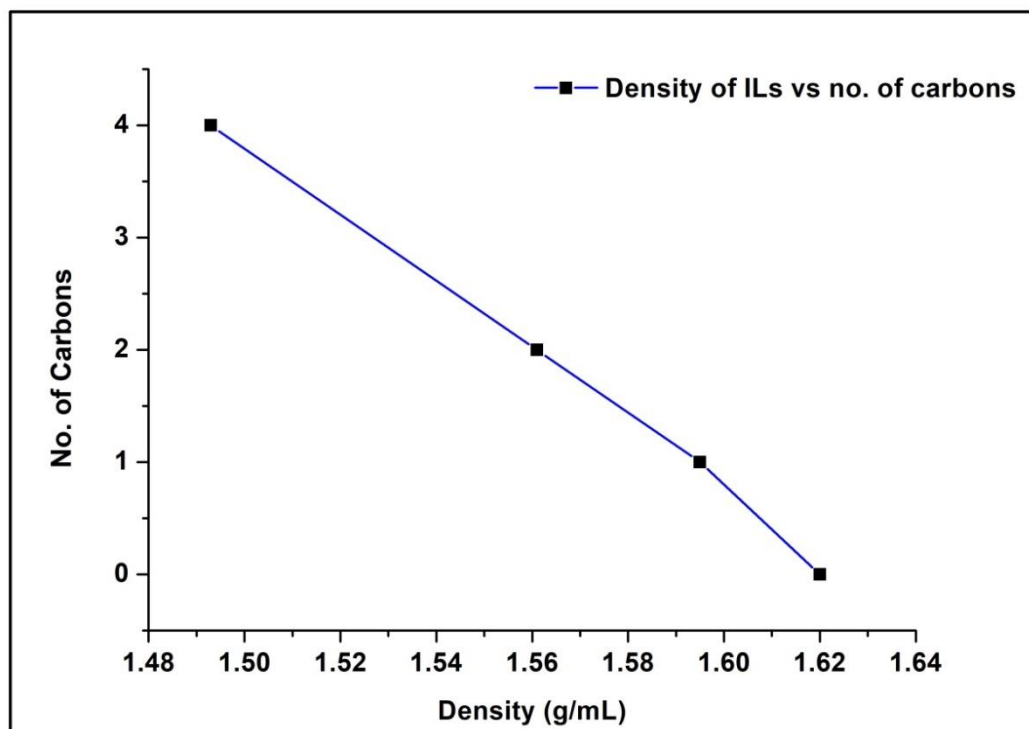
Fig. 3.5: Density of the ILs vs number of carbons in the alkyl side chain.

3.2.2.4 Conductivity study of BAILs in molecular solvents

The conductivity (σ) of the four 1, 3-disulfoimidazolium trifluoroacetate ILs [RSIM][TFA] were measured in two molecular solvents methanol (MeOH) and acetonitrile (MeCN) by varying the temperature and concentration of the ILs.

Effect of ionic liquid concentration

The binary mixture of ionic liquid and molecular solvent is supposed to exhibit substantially higher electrical conductivity than pure ionic liquids due to the presence of large number of charge carriers in the mixtures and decreased viscosity. The typical N-SO_3H functionalized imidazolium ILs have the potential to possess surface active properties similar to the surfactants and would therefore allow them to form aggregates or micelles in solutions [20]. Each of the ion-pair of these acidic ILs could form two types of domain: the first one consisting of positively charged cations and negatively charged anions arranging in three-dimensional polar networks supported by strong electrostatic interactions, and the second one comprising of hydrophobic alkyl groups aggregating to form non-polar domains where short-range van der Waals interactions are predominant tail domain as shown in **Fig. 3.6**. So, they have a tendency to organize themselves into aggregates differently in molecular solvents depending on the length of

the hydrophobic tail. It was seen that at a given temperature, the conductivity of ILs in molecular solvent rises slowly with the increasing mole fraction of the IL up to a certain concentration due to the increase in the number of charge carriers (free ions). Above that concentration, the conductivity of IL decreases gradually till it gets a minimum value with its neat condition.
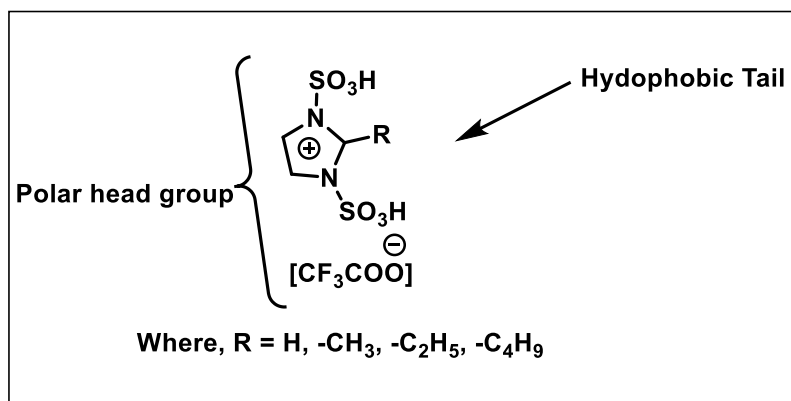
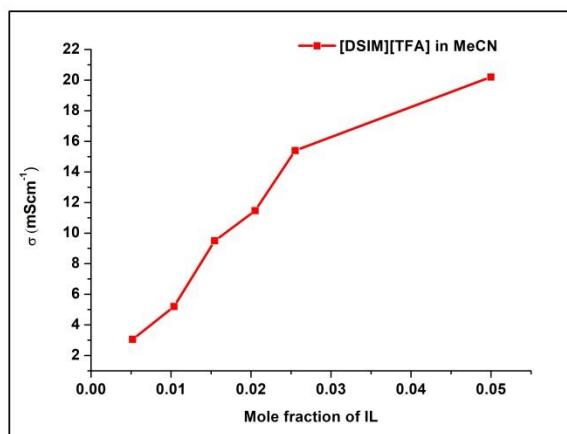**Fig. 3.6:** Hydrophilic head group and hydrophobic domain of 2-alkylsubstituted imidazolium IL.

This variation in the conductivity of the imidazolium IL-molecular solvent binary mixtures can be explained by considering two factors: (1) aggregation tendency of the IL molecules above the "Critical Aggregate Concentration (CAC)" and (2) the increasing viscosity of the IL solution. Several other factors such as bulkiness of the alkyl substituent and its branching, polar or non-polar nature of the molecular solvents, solution temperature etc. may also function together to control the sizes of the aggregates of ILs in molecular solvents. In this study, we can expect the sizes of the aggregates of IL molecules in the molecular solvents to be smaller compared to the surfactants due to shorter chain length of the alkyl groups. Further, polar solvents are favorable for the formation of smaller sized aggregates of ILs as compared to non-polar solvents [47], hence the conductivity of each of the $-SO_3H$ functionalized ILs at a particular concentration and temperature in its solution in MeOH is more than that in its solution in MeCN. The conductivity (σ) of the binary mixture of the ionic liquids [DSIM][TFA], [MDSIM][TFA], [EDSIM][TFA] and [BDSIM][TFA] in MeCN and MeOH were measured at room temperature by varying the mole fraction of the ILs within $X_{IL} = 0.005$ to $X_{IL} = 0.2$ (**Table 3.4**).The corresponding graphical expression of conductivity vs mole fraction of the ILs is included in **Fig. 3.7**. These graphs also displayed an increase in the

conductivity values of the binary mixtures with the increasing mole fraction of the ILs at a particular temperature (298.15 K) below their "CAC" values.
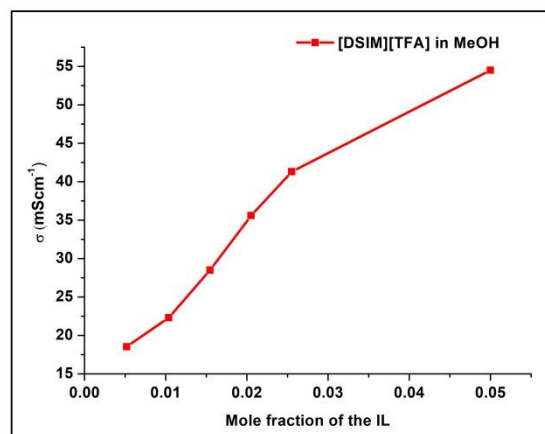
The existence of CAC values of these binary mixtures of IL-molecular solvents were further evidenced with a representative study of the [MDSIM][TFA] ionic liquid in MeOH by measuring the conductivity of this IL-MeOH binary mixture up to the mole fraction of X_{IL}=0.2 at room temperature (**Fig. 3.7(D)**). As expected the conductivity of [MDSIM] [TFA] mixture in MeOH increased with the increasing concentration of the IL from X_{IL}=0.0052 to X_IL=0.05. However, the increase in conductivity values in between X_{IL}=0.05 to X_{IL}=0.1wasn't much steeper. Above the mole fraction of 0.1, the conductivity values showed a sharp decrease at X_{IL} = 0.15. This can be attributed to the reduction in the number of free charge carriers at high concentration of the ILs due to aggregate formation and thus, decreasing the conductivity of the binary mixtures of IL-molecular solvent [48].

Table 3.4: Conductivity of the ILs in MeOH and MeCN with their varying mole fraction (X_{IL}) at 298.15 K.

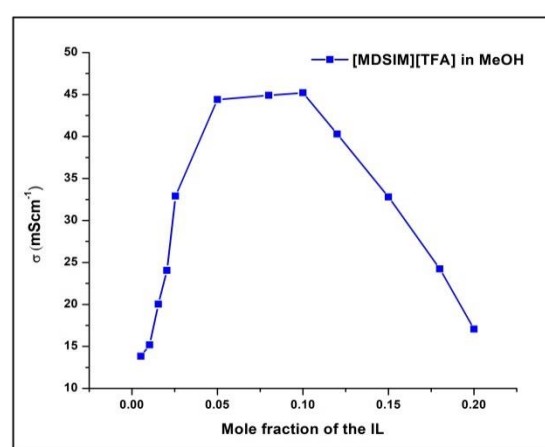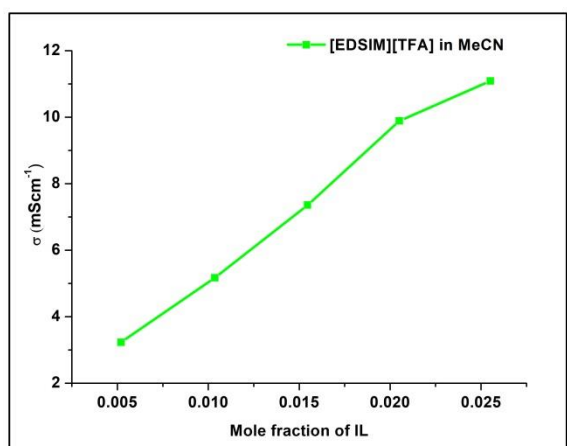| Mole fraction of IL	[DSIM][TFA] $\sigma(mScm^{-1})$		[MDSIM][TFA] $\sigma(mScm^{-1})$		[EDSIM][TFA] $\sigma(mScm^{-1})$		[BDSIM][TFA] $\sigma(mScm^{-1})$	
	MeOH	MeCN	MeOH	MeCN	MeOH	MeCN	MeOH	MeCN
0.0052	18.53	3.05	13.83	3.51	15.12	3.23	14.10	3.59
0.0104	22.30	5.20	15.18	5.28	16.38	5.17	15.89	4.25
0.0155	28.50	9.49	20.03	6.98	19.27	7.36	17.56	5.54
0.0205	35.60	11.47	24.06	10.38	22.70	9.89	21.57	6.32
0.0255	41.30	15.40	32.90	12.59	30.80	11.09	26.50	8.99
0.0500	54.50	20.20	44.40					
0.0800			44.90					
0.1000			45.20					
0.1200			40.29					
0.1500			32.80					
0.1800			24.24					
0.2000			17.06					

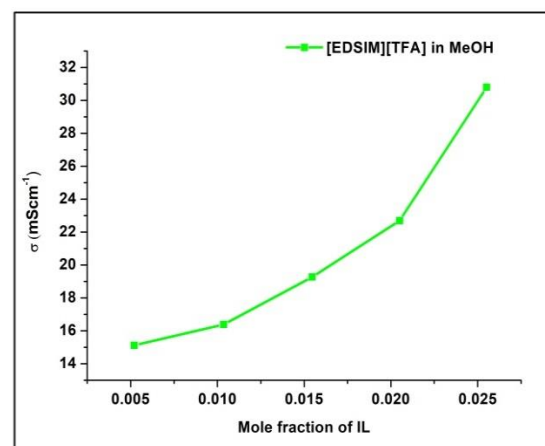(A)

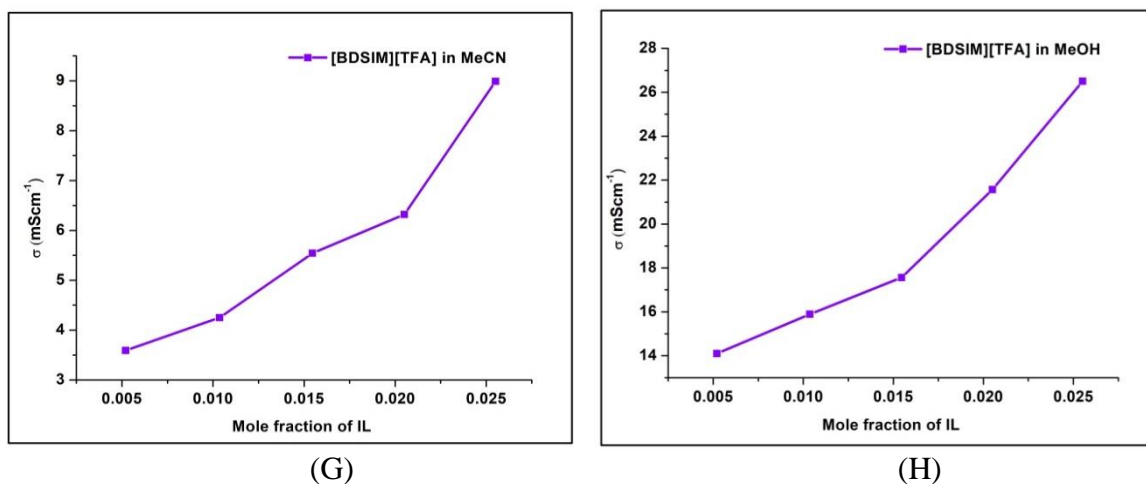(B)

(C)

(D)

(E)

(F)

(G)   (H)
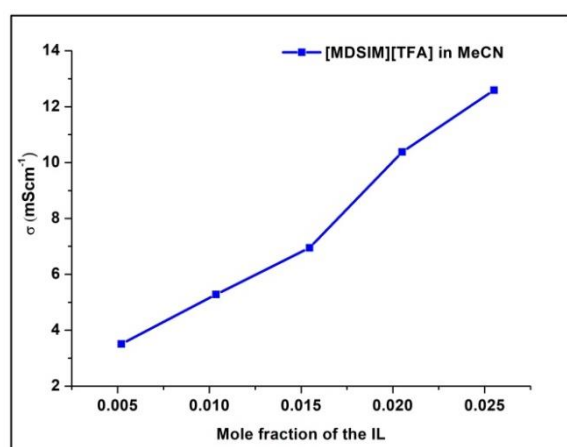
Fig. 3.7: Plot of conductivity vs concentration of ionic liquids: (A) [DSIM][TFA] in MeCN, (B) [DSIM][TFA] in MeOH, (C) [MDSIM][TFA] in MeCN, (D) [MDSIM][TFA] in MeOH,(E) [EDSIM][TFA] in MeCN, (F) [EDSIM][TFA] in MeOH (G) [BDSIM][TFA] in MeCN, (H) [BDSIM][TFA] in MeOH.

Effect of temperature

The effect of temperature on the conductivity (σ) of each of the four BAILs at a particular mole fraction $X_{IL} = 0.0255$ was investigated in the temperature range 278.15 K to 333.15 K, in both methanol and acetonitrile as shown in **Table 3.5** and **Fig. 3.8**. The conductivity values of the ILs were found to decrease with increasing temperature. This indicates the existence of some type of dynamic equilibrium of the smaller sized aggregates of ILs with the bulkier ones under thermodynamic condition in methanol and acetonitrile [20, 48]. As the temperature increases, the smaller aggregates gain more energy and tend to come closer to form stable aggregates of bigger sizes. This reduces the number of free charge carriers and hence the conductivity (σ) of ionic liquid mixtures with molecular solvent decreases with increasing temperature.

Effect of the cation size

The σ values (**Table 3.4**) of binary mixtures of these four ILs in both the molecular solvents decreased in the following order: [DSIM][TFA]>[MDSIM][TFA]>[EDSIM][TFA] >[BDSIM][TFA]. This was in opposite order to the increasing sizes of C-2 alkyl group of the imidazolium cation i.e.: H<Me<Et<n-Bu. Since, the increasing bulkiness of C-2 alkyl substituent decreases the mobility of the imidazolium cation in both the solvents studied, so the conductivity of IL

solutions is lowered in both the cases [20]. **Fig. 3.9** shows the plot of conductivity of the ILs (X_{IL} = 0.2551, 298.15 K) vs the number of carbons in the alkyl chain length of the cations in MeOH and MeCN.

Table 3.5: Conductivity of the ILs in MeOH and MeCN (X_{IL} =0.0255) in the temperature range 278.15-333.15 K.

| Temperature (K)	[DSIM][TFA] $\sigma(mScm^{-1})$		[MDSIM][TFA] $\sigma(mScm^{-1})$		[EDSIM][TFA] $\sigma(mScm^{-1})$		[BDSIM] [TFA] $\sigma(mScm^{-1})$	
	MeOH	CH$_3$CN	MeOH	CH$_3$CN	MeOH	CH$_3$CN	MeOH	CH$_3$CN
278.15	51.90	18.30	42.9	13.87	37.50	12.16	31.81	12.36
283.15	49.00	17.79	40.00	13.65	35.70	12.09	30.10	11.90
288.15	46.40	16.20	36.40	13.01	34.40	12.01	28.93	10.72
293.15	42.60	15.90	35.50	12.89	32.80	11.14	27.17	9.44
298.15	41.30	15.40	32.90	12.59	30.80	11.09	26.52	8.99
303.15	40.46	12.67	30.10	12.01	30.30	8.23	24.50	6.65
308.15	38.90	12.52	29.80	11.49	29.50	8.24	22.80	6.46
313.15	37.60	12.49	28.60	11.04	27.00	8.16	20.76	5.45
318.15	35.20	12.47	28.40	10.93	25.10	7.67	19.11	5.21
323.15	34.60	8.03	27.30	10.77	23.60	7.55	17.30	4.68
328.15	33.70	4.86	26.30	7.06	21.90	6.89	16.92	4.57
333.15	32.50	4.01	23.20	6.16	19.60	6.52	15.74	4.23

Effect of solvatochromic parameters

Physicochemical properties of pure ILs like viscosity, density, electrical conductivity, solubility, solvation as well as its reactivity are directly influenced on addition of any co-solvent. Additionally, intermolecular H-bond formation ability of the protic co-solvents with the constituent ion-pair of IL enhances the electrical conductivity of the binary mixtures of IL-molecular solvents by stabilizing the free charged species. The conductivities of the ionic liquid-molecular solvent binary mixtures are often affected by the nature of the solvent. The variation of conductivity of ionic liquids in molecular solvents can be expressed as a function of the Kamlet-Taft solvatochromic relationship which describes the contribution of hydrogen bond donor(α), hydrogen bond acceptor (β)
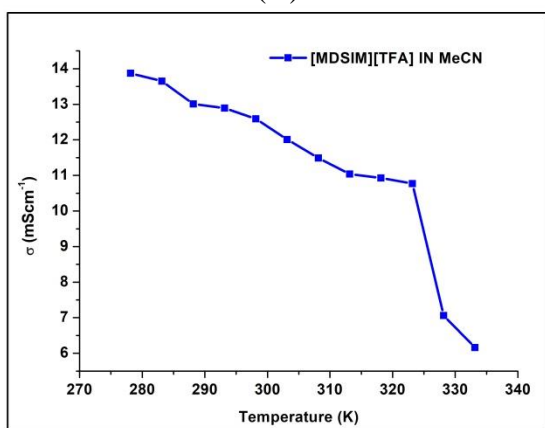
properties of solvents and Dimroth-Richardt's $E^T(30)$ values to the overall solvent polarity of solution [20,32, 39].
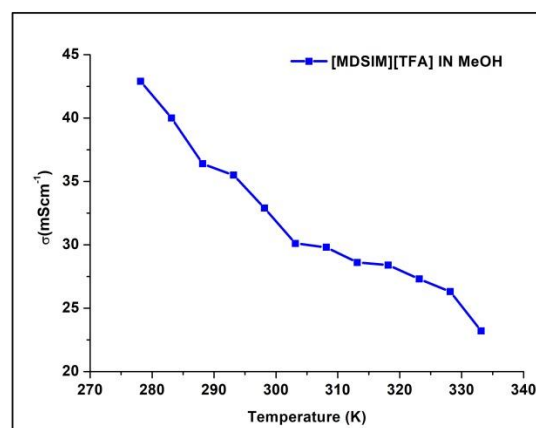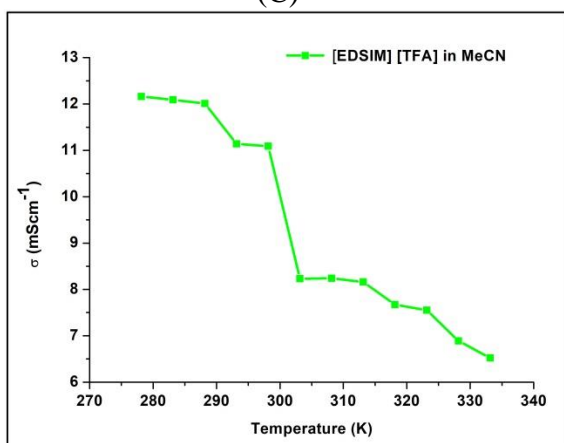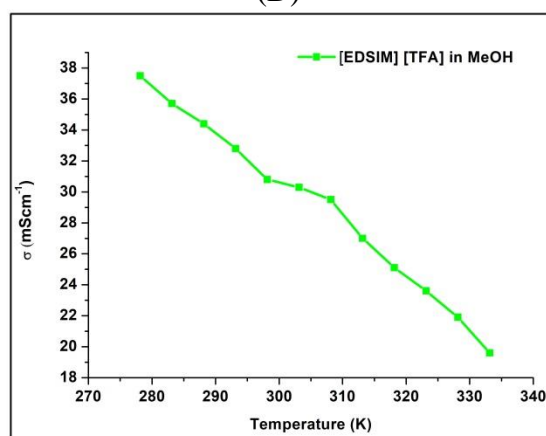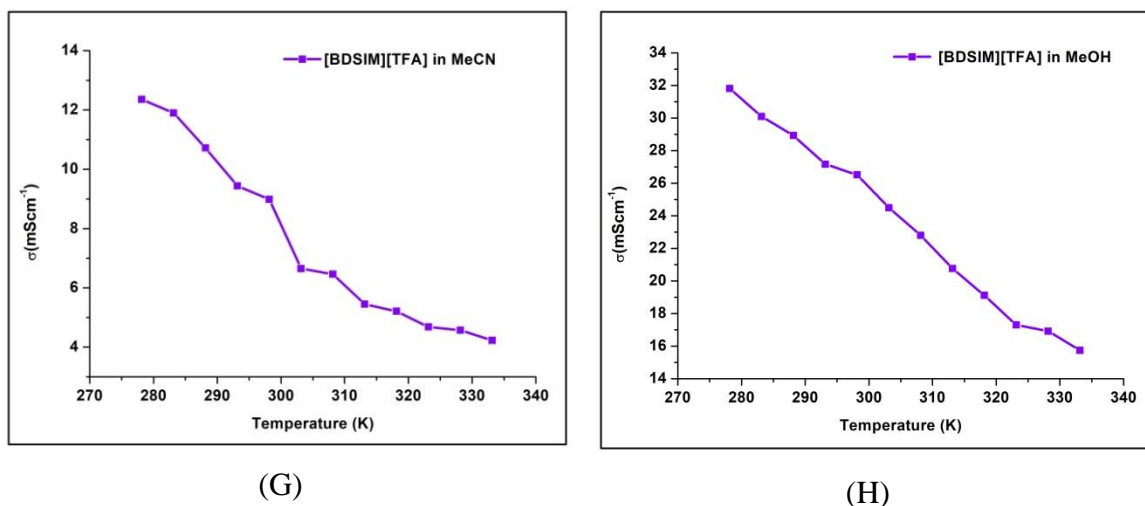

(A)

(B)

(C)

(D)

(E)

(F)

(G)

(H)
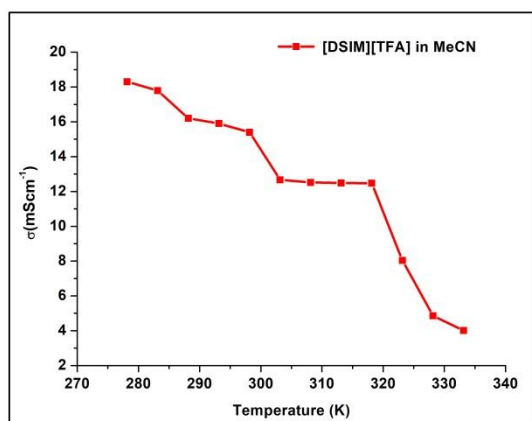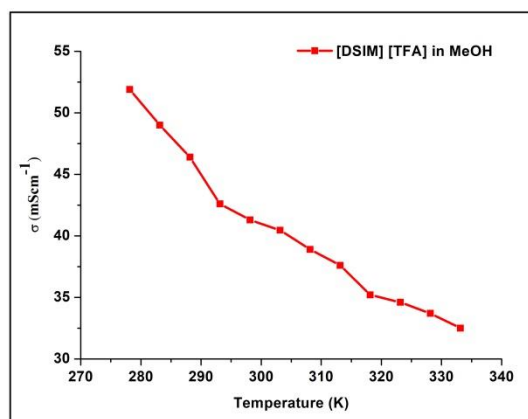
Fig. 3.8: Plot of Conductivity of Ionic liquid-molecular solvent binary mixture vs temperature of (A) [DSIM][TFA] in MeCN, (B) [DSIM][TFA] in MeOH, (C) [MDSIM][TFA] in MeCN,(D) [MDSIM][TFA] in MeOH, (E) [EDSIM][TFA] in MeCN, (F) [EDSIM][TFA] in MeOH (G) [BDSIM][TFA] in MeCN, (H) [BDSIM][TFA] in MeOH.

To predict the polarity of solvents based on solvent-solute interactions the empirical Kamlet-Taft empirical polarity scale was developed involving three fundamental physical properties: (a) cavity formation that takes into account of dispersive forces, (b) dipolar interactions (π^*) such as dipole-dipole and dipole-induced dipole forces and (c) H-bond donor (α) / acceptor ability (β).
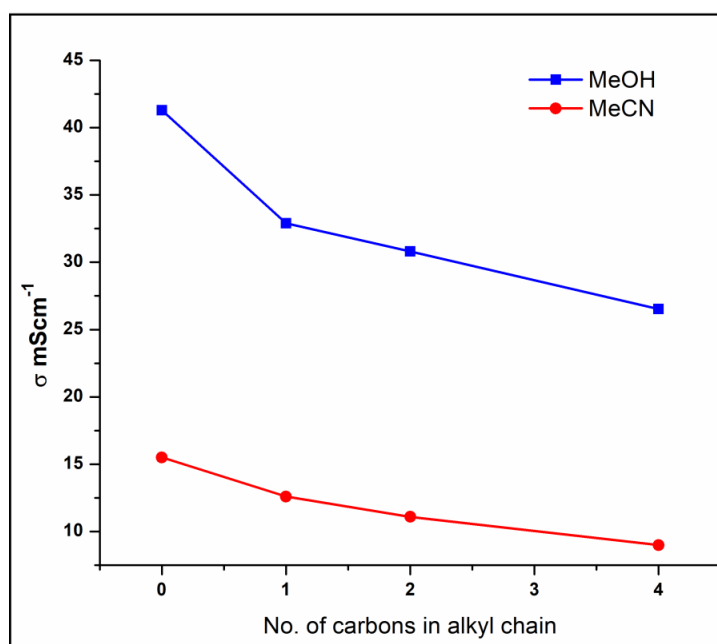
Fig. 3.9: A plot of σ vs the alkyl chain length of the cations of ILs in MeOH and MeCN.

The partial contribution of each parameter is expressed in **Equation 3.1.**

$$P = P_0 + A\,(\partial_1)^2 V_2 + B{\cdot}\pi_1\pi_2 + C{\cdot}\alpha_1\beta_2 + D\,\alpha_2\beta_1 \qquad \textbf{(Equation 3.1)}$$

Here the subscript 1 and 2 refers to the solvent and solute components. This equation utilizes the Hildebrand's solubility parameter (∂) and molar volume of the solute (Vm) for determination of the cavity term.

The polarity parameters of solvents are obtained from UV-Vis spectroscopy of selected probe molecules in terms of "solvatochromic effects''. This term is used to describe the change in the position of UV-Vis maximum (λ_{max}) absorption band of the probe on the basis of their differences in solvation free-energy of ground and excited states. It is observed that the polarity of solvents also affects the intensity and shape of the absorption band. The absorption peak shifts to shorter wavelength (hypsochromic shift) as the polarity of solvent increases, thus lowering of the solvation free energy. A bathochromic shift (shift to longer wavelength) is observed as the polarity of solvent reduces. The betaine dye E_T (30) is used as a polarity indicator and it acts as a strong solvatochromic probe for the UV-Vis experiment. The empirical Dimroth-Reichardt polarity scale E_T (30), of various solvents is simply defined as the molar transition and is expressed according to **Equation 3.2**.

$$E_T(30)/\,kcal\;mol^{-1} = hc\;\bar{\upsilon}_{max}\,N_A = (2.8591*10^{-3})\;\bar{\upsilon}_{max}\,/cm^{-1} = 28591\,/(\lambda_{max}/nm)$$

$$\textbf{(Equation 3.2)}$$

$$E^T{}_{N} = (E_T(30) - 30.7)/\,32.4$$

$$\textbf{(Equation 3.3)}$$

Similarly, the $E^T{}_N$ scale express solvent polarity arising from overall interactions between a solvent and the dye. The normalized $E^T{}_N$ polarity is obtained by measuring the wavelength corresponding to maximum absorption in a solvent and is related to the E_T (30) values of the solvent according to **Equation 3.3.** Here E_T (30) in kcal mol^{-1} is 28591/ (λ_{max} /nm); where, λ_{max} is the wavelength corresponding to maximum absorption.

In this case, the known solvatochromic parameter values (**Table 3.6**) of MeOH and MeCN were utilized for analyzing the variation in conductivity (**Table 3.7**) of the four ILs in the molecular solvents (**Fig. 3.10**) at the mole fraction of x_{IL}=0.0255 at 298.15 K [32, 39].The conductivity (σ) of ionic liquid solutions increases with increasing polarity of the molecular solvent represented with the values of E^T_N in increasing order of MeCN<MeOH in **Fig. 3.10(A)**.The possible H-bonding interactions of the –SO_3H groups of these ILs with the molecules of protic solvent (MeOH) are mostly responsible for greater stability of the constituent ion-pairs of the ILs in the MeOH compared to the aprotic polar solvent like MeCN. Thus, the solvation of cations and anions of the ILs in these solvents are mainly controlled by the hydrogen-bond donor ability (α) of the solvent which plays a crucial role in their conductivity [34]. The high H-bond donor ability of MeOH increased the conductivity values of the binary mixtures of the IL solution in **Fig. 3.10(B)**. Similarly, the H-bond acceptor properties (β) of the medium also affect the conduction behavior of the ILs solution. The σ values decreases with the decrease of H-bond acceptor values (β) of the solvents (**Fig. 3.10(C)**).

Table 3.6: Solvatochromic parameters of MeOH and MeCN at 298.15 K.

Solvent	E^T_N	α	β
MeOH	0.762	1.05	0.61
MeCN	0.460	0.38	0.39

Table 3.7: Conductivity of IL solutions with mole fraction x_{IL}= 0.0255 at 298.15 K.

Ionic liquids	Conductivity (mS cm^{-1})	
	MeOH	MeCN
[DSIM][TFA]	41.30	15.40
[MDSIM][TFA]	32.90	12.59
[EDSIM][TFA]	30.80	11.09
[BDSIM][TFA]	26.52	8.99
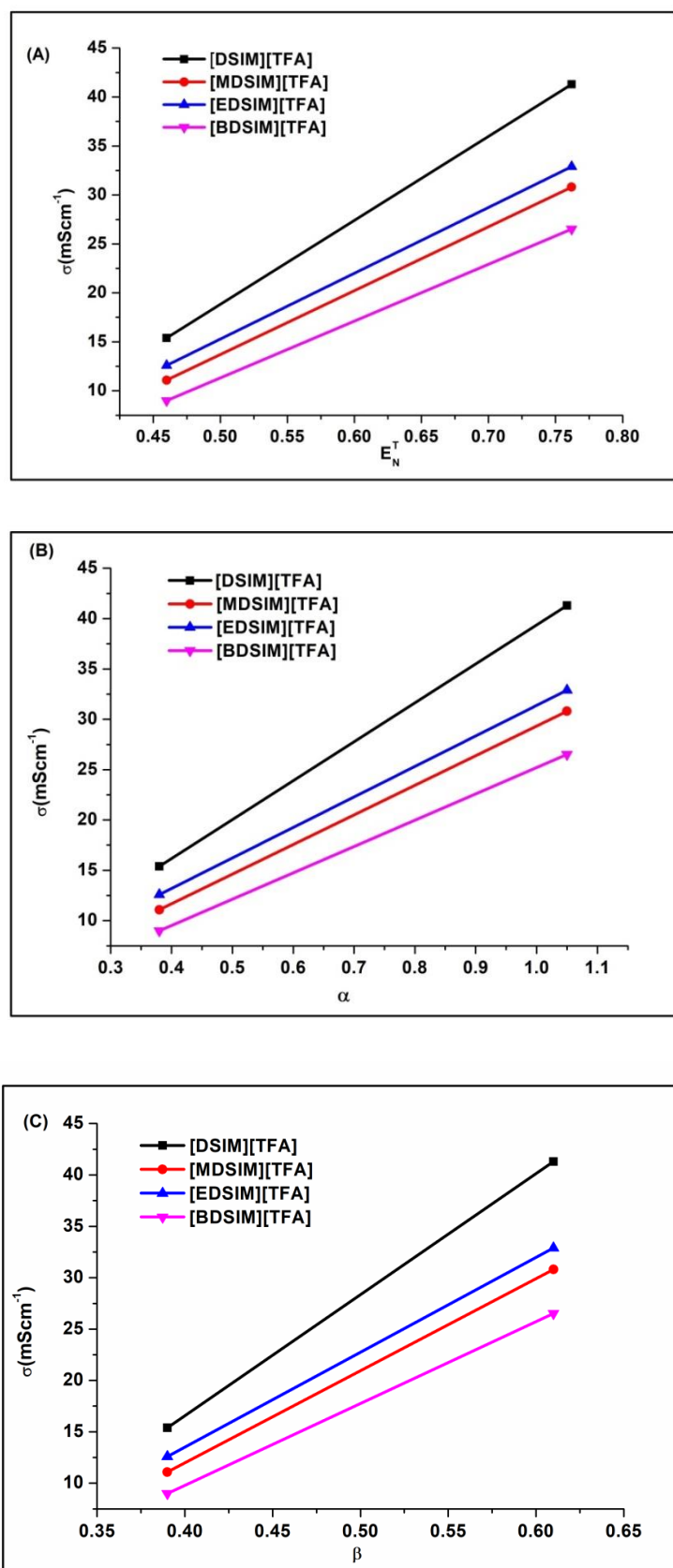
Fig. 3.10: Plot of (A) Conductivity of ILs vs E^T_N. (B) Conductivity of ILs vs α. (C) Conductivity of ILs vs β.

3.2.2.5 Electrochemical stability of ionic liquids in molecular solvents

The cyclic volatmmograms (CVs) of 0.1 M solution of the ionic liquids in MeOH (or MeCN) were recorded at room temperature using glassy carbon as the working electrode and Ag/AgCl as the reference electrode. The electrochemical windows of the ionic liquids were calculated using **Equation 1.3** from **chapter 1**. The calculated electrochemical stability windows of the binary mixtures of ILs are included in **Table 3.8** corresponding to their CV plots in **Fig.3.11**.

$$ESW = E_{anodic} - E_{cathodic} \qquad \textbf{(Equation 1.3)}$$

It was found that the electrochemical stability of the ion-pairs of four ionic liquids in molecular solvents is affected by the variation of solvent-solute interactions. The electrochemical windows of all the four BAILs were narrowed on both cathodic and anodic sites for their solution in methanol. This can be accounted for the possible electrochemical oxidation of the CF_3COO^- anion to radical intermediate, followed by abstraction of hydrogen radical from the protic MeOH solvent to produce CF_3COOH molecule. In case of acetonitrile, the lack of acidic proton in the solvent was found favourable for increasing the anodic potential limits of CF_3COO^- anion to 1.755–1.862 V from the range of 1.493–1.499 V in methanol. The +I effect of the C-2 alkyl substituents doesn't influence the cathodic limits which is supported by the similar cathodic potential of the 2-alkyl 1,3-disulfoimidazolium cations around 0.285–0.298 V in methanol. The oxidative decomposition of the trifluoroacetate anion primarily determines almost the identical ESWs of the ILs in methanol solution. The lowering of cathodic limit of the [DSIM][TFA] in acetonitrile is related to the acidity of C-2 proton of the imidazolium ring for reduction of the1,3-disulfoimdazolium cation through radical and carbene formation [3]. Dimerization of the radical species leads to formation of dimers or disproportionation with other imidazolium species to form a compound containing saturated C2 carbon [49].For the [MDSIM][TFA] ionic liquid, the presence of three acidic protons in the C-2 methyl group may accelerate the initial reductive elimination of side chain from the imidazolium cation and thus, minimize the cathodic potential in acetonitrile. Replacing the methyl substituent by ethyl substituent in the [EDSIM][TFA] and n-butyl substituent in the [BDSIM][TFA] increases the reductive stability of the corresponding imidazolium cations by electron donating inductive effect [15, 16, 31]. As an outcome of this effect, we got slight variation of the cathodic limit values at −0.850 V
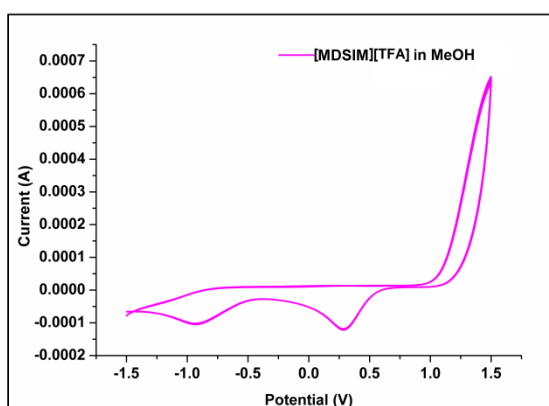
and −0.862 V for the [EDSIM] [TFA] and [BDSIM][TFA] respectively in acetonitrile leading to higher ESWs of these ILs. Thus, it can be concluded that the ESWs of these ILs in acetonitrile are mostly controlled by the reductive potential of the imidazolium cations.
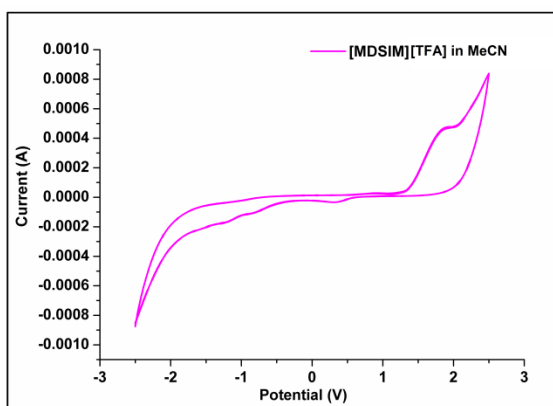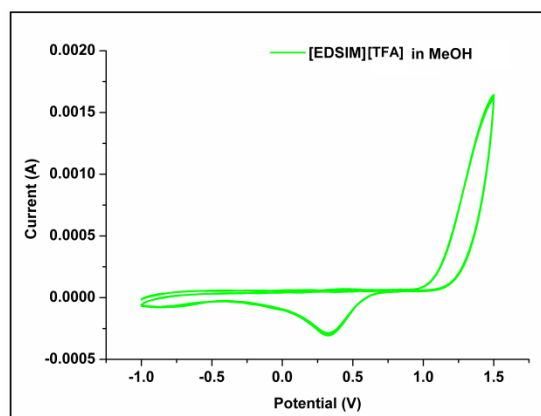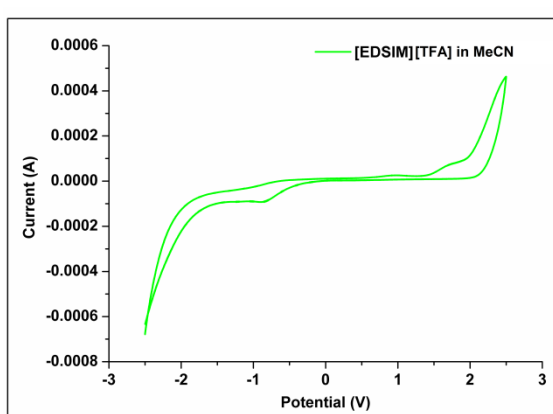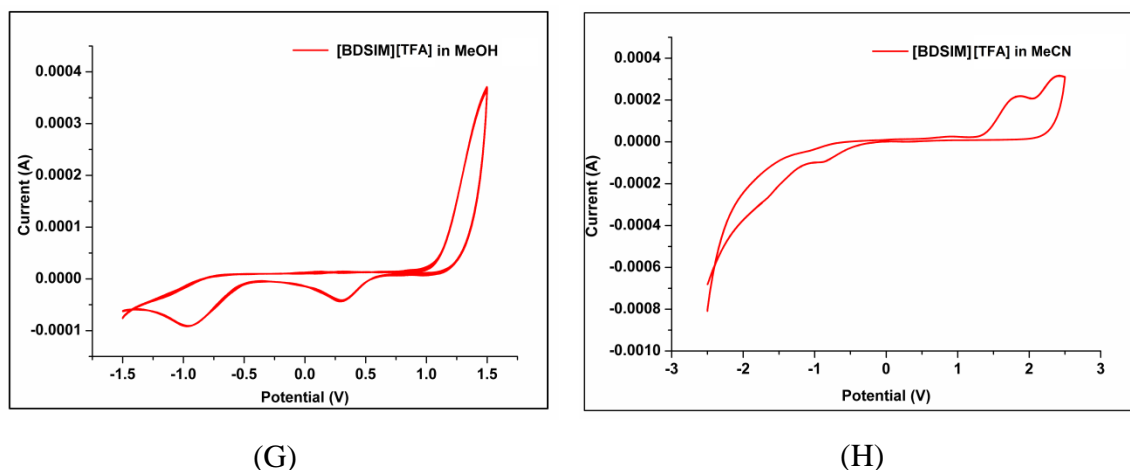

(A)

(B)

(C)

(D)

(E)

(F)

(G)

(H)
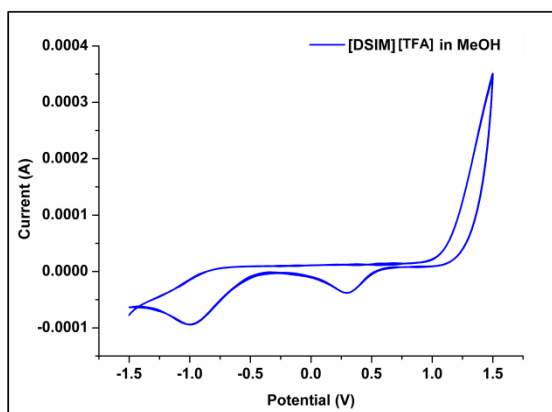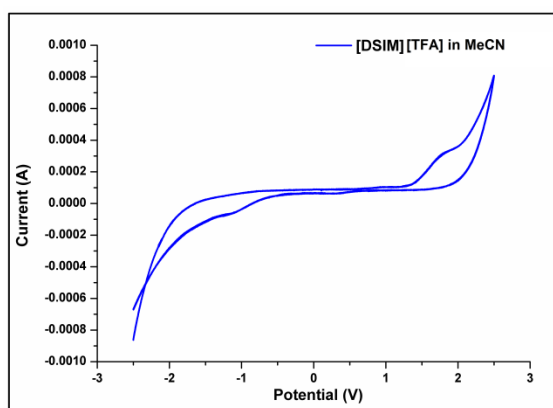
Fig. 3.11: Cyclic Voltammograms of the ionic liquids: (A) [DSIM][TFA] in MeOH, (B) [DSIM][TFA] in MeCN, (C) [MDSIM][TFA] in MeOH, (D) [MDSIM][TFA] in MeCN, (E)[EDSIM][TFA] in MeOH, (F) [EDSIM][TFA] in MeCN (G) [BDSIM][TFA] in MeOH, (H) [BDSIM][TFA] in MeCN.

Table 3.8: ESW of the ILs calculated from the observed cathodic and anodic potentials.

Ionic liquids	Solvent (MeOH)			Solvent (MeCN)		
	Anodic potential (E_{anodic})	Cathodic Potential ($E_{cathodic}$)	Electrochemical window (ESW)	Anodic potential (E_{anodic})	Cathodic Potential ($E_{cathodic}$)	Electrochemical window (ESW)
[DSIM] [TFA]	1.493	0.298	1.195	1.755	0.328	1.427
[MDSIM] [TFA]	1.499	0.285	1.198	1.862	0.306	1.556
[EDSIM] [TFA]	1.497	0.291	1.206	1.755	-0.850	2.605
[BDSIM] [TFA]	1.499	0.298	1.208	1.842	-0.862	2.704

3.3 Summary

In this work, four members of N-SO$_3$H functionalized Brønsted acidic 2-alkyl-1,3-disulfoimidazolium trifluoroacetate ILs were synthesized and were subjected to the analysis of their physical and electrochemical properties after their characterization by ^{1}H NMR, ^{13}C NMR, FT-IR and elemental analysis techniques. It was found that their densities and Hammett acidities reduced on increasing the chain length of the C-2 alkyl substituent. All the four BAILs were found to be thermally stable up to 250–260 °C. Their hydrophilic nature was dependent on the C-2 substituent of the imidazolium cation. Self-aggregation tendency of the ILs molecules in presence of the molecular solvents (MeOH & MeCN) was responsible for the reduction of the conductivity values of the IL solutions at a particular mole fraction with the rise in temperature. The measurement of the conductivities of [MDSIM][TFA] in MeOH by varying the concentration of the (X_{IL} = 0.0052 to 0.2) at room temperature indicated the existence of "Critical aggregation concentration" around X_{IL} = 0.1 (**Fig. 3.7D**). Additionally, the BAILs showed higher conductivities in MeOH compared to MeCN at a constant temperature (298.15 K) and concentration (X_{IL} = 0.0255) due to the H-bonding stabilizing effects of the free charged species in MeOH. Cyclic Voltammetry study revealed wider ESWs of the BAILs in MeCN compared to MeOH at the same temperature. The wider ESWs C-2 ethyl and n-butyl substituted 1,3-disulfoimidazolium trifluoroacetate ILs in MeCN were found to be the result of the enhancement of electron donating inductive effects of the alkyl groups. This study reveals the possible extension of this work with other types of the N-SO$_3$H functionalized organic cations containing ILs with high conductivity, thermal, chemical, acidity and electrochemical stability, making them suitable candidates as catalysts, electrolyte material in various electrochemical devices in their pure state or as a binary mixture with molecular solvents.
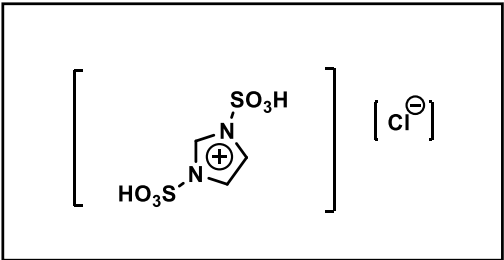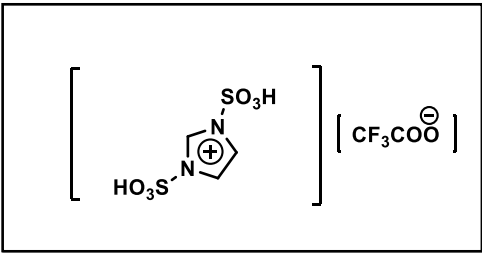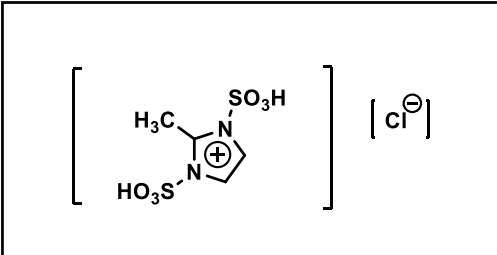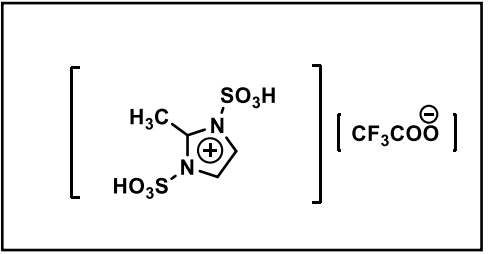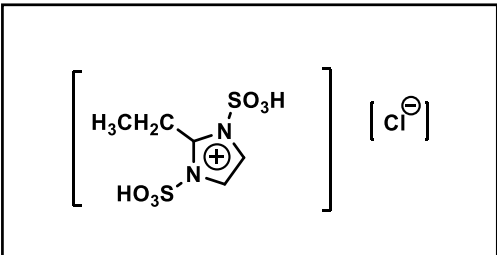
3.4 Experimental Section

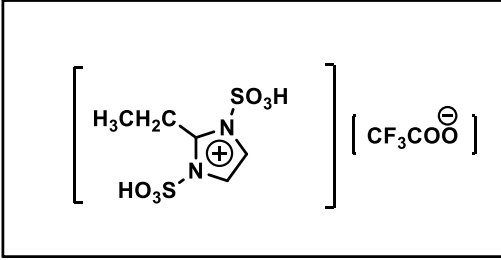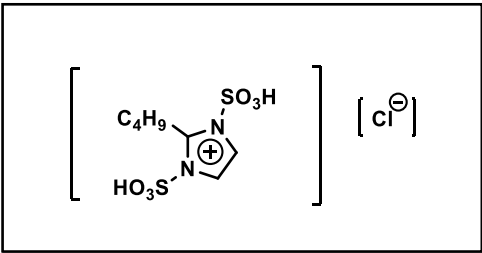### 3.4.1 Synthesis of the N-SO$_3$H functionalized Brønsted acidic ionic liquids (BAILs)
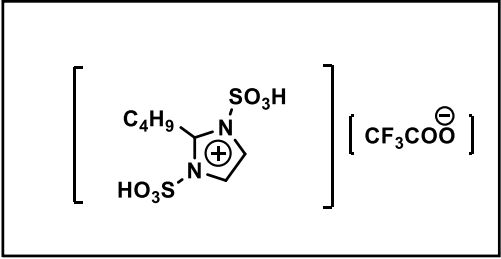
The N-SO$_3$H functionalized ionic liquids [RSIM][TFA], where R = H, CH$_3$, C$_2$H$_5$ and n-C$_4$H$_9$ were prepared following the standard procedure in a two-step method (**Scheme 3.1**) [1]. The first step involves dissolving 20 mmol of imidazole or substituted imidazole in 10 mL of dry DCM (CH$_2$Cl$_2$) in a two neck 100 mL round bottomed flask. It was then

stirred for few minutes. Then chlorosulfonic acid (40 mmol) was added drop wise to the stirred solution of imidazole or substituted imidazole in DCM over a period of 3 min at ice-cold conditions to prepare the initial ionic liquid [RSIM][Cl]. It was then stirred at room temperature for 30 minutes. The DCM was evaporated in rotary evaporator to isolate the viscous chloride based [RSIM][Cl] IL. In the second step, 20 mmol of CF_3COOH was added to the parent ionic liquid [RSIM][Cl] (20 mmol) at 80 °C and was stirred for 2 hours to produce the corresponding anion exchanged trifluoroacetate ionic liquids [RSIM][TFA]. The HCl gas outlet was connected to a vacuum system through water and an alkali trap. The crude IL was washed with dry DCM (3×5 mL) in which it is immiscible and then decanted to get the analytically pure ionic liquid.

### 3.4.2 Spectral data of the N-SO₃H functionalized BAILS

Sl No.	Ionic liquid	Spectral data
1	 1,3-disulfoimidazolium chloride [DSIM][Cl]	Yellow viscous liquid; FT-IR (KBr) υ cm⁻¹: 3433, 3351,1591, 1523, 1436, 1045, 875.4, 757, 617, 585, 455 and 437; ¹H NMR (DMSO-d_6, 400 MHz): δ 14.35 (s, 1H), 13.23-13.04 (m, 1H), 9.00 (s, 1H), 7.72-7.57 (m, 2H); ¹³C NMR (DMSO-d_6, 100 MHz) : δ 135.2, 120.5 and 119.9; CHN analysis(%): Cal. C 13.46, H 3.01, N 10.47; Found C 13.43, H 3.05, N 10.42.
2	 1,3-disulfoimidazolium trifluoroacetate [DSIM][TFA]	Brown viscous liquid; FT-IR (KBr) υ cm⁻¹: 3420, 3376, 1709, 1641, 1178, 1054,875 and 587; ¹H NMR (DMSO-d_6, 400 MHz): δ 14.15 (s, 1H), 13.42 (s, 1H), 9.05-8.88 (m, 1H), 7.60-7.48 (m, 2H);¹³C NMR (DMSO-d_6, 100 MHz): δ 158.5, 136.7, 134.6, 119.6 and 62.37; CHN analysis(%): Cal. C 17.40, H 2.34, N 8.11; Found C 17.46, H

		2.39, N 8.08.
3	 2-methyl-1,3-disulfoimidazolium chloride [MDSIM][Cl]	Yellow viscous liquid; FT-IR (KBr) υ cm⁻¹: 3425, 3067, 2917, 1627, 1445,1191,1050, 873, 753 and 580; ^{1}H NMR (DMSO-d$_6$, 400 MHz): δ 13.91 (s, 1H), 11.93 (s, 1H), 7.43 (s, 2H), 2.51 (s, 3H); ^{13}C NMR (DMSO-d$_6$, 100 MHz) : δ 144.9, 119.1 and 11.3; CHN analysis(%) :Cal. C 17.05, H 3.58, N 9.94; Found C 17.11, H 3.54, N 9.90.
4	 2-methyl-1,3-disulfoimidazolium trifluoroacetate [MDSIM][TFA]	Brown viscous liquid; FT-IR (KBr) υ cm⁻¹: 3445, 3016, 2910,1748, 1627, 1445, 1198, 1054, 881, 756 and 585; ^{1}H NMR (DMSO-d$_6$, 400 MHz): δ 13.91 (s, 1H), 12.96 (s, 1H), 7.47-7.41 (m, 2H), 2.51 (s, 3H); ^{13}C NMR (DMSO-d$_6$, 100 MHz) : δ 159, 144.9, 118.3 and 11.7; CHN analysis(%) :Cal. C 20.06, H 2.81, N 7.80; Found C 20.10, H 2.74, N 7.93.
5	 2-ethyl-1,3- disulfoimidazolium chloride [EDSIM][Cl]	Yellow viscous liquid; FT-IR (KBr) υ cm⁻¹ : 3437,2929, 2860, 1629, 1453, 1176, 1054, 872, 750, 581; ^{1}H NMR (DMSO-d$_6$, 400 MHz): δ 13.94 (s, 1H) 13.0 (s, 1H), 7.47-7.42 (m,2H), 2.88-2.84 (m, 2H), 1.24-1.17 (m, 3H); ^{13}C NMR (DMSO-d$_6$, 100 MHz): δ 149.1, 119.1, 19.2 and 11.7; CHN analysis(%) : Cal. C 20.31, H 4.09, N 9.47; Found C 20.25, H 4.11, N 9.60.
6		Brown viscous liquid; FT-IR (KBr) υ cm⁻¹: 3448, 2923, 2853,1760, 1626, 1451, 1184, 1060, 884, 758 and 585;

	2-ethyl-1, 3- disulfoimidazolium trifluoroacetate [EDSIM][TFA]	^{1}H NMR (DMSO-d_6, 400 MHz): δ 13.8 (s, 2H), 7.47 (s, 2H), 2.88 (q, J = 8 Hz, 2H), 1.22 (t, J = 8.0 Hz, 3H); ^{13}C NMR (DMSO-d_6, 100 MHz) : δ 159.2, 148.4, 119.1, 19.2 and 11.7; CHN analysis(%) :Cal. C 22.52, H 3.24, N 7.50; Found C 22.47, H 3.36, N 7.62.
7	2-butyl-1, 3-disulfoimidazolium chloride [BDSIM][Cl]	Yellow viscous liquid; FT-IR (KBr) υ cm^{-1}: 3419, 3154, 2961, 2936, 2839, 2376, 1725, 1625, 1460, 1301, 1243, 1165, 1037, 876, 753, 573 and 444; ^{1}H NMR (400 MHz, DMSO-d_6): δ 13.17 (s, 1H), 7.40 (s, 2H), 2.84 (t, J = 8.0 Hz, 2H), 1.63-1.59 (m 2H), 1.21-1.16 (m, 2H), 0.79 (t, J = 8.0 Hz, 3H); ^{13}C NMR(100 MHz, DMSO-d_6): δ 148.2, 119.2, 29.3, 25.0, 21.4 and 13.6; CHN analysis(%) : Cal. C 25.97, H 4.98, N 8.65; Found C 25.91, H 4.83, N 8.60.
8	2-butyl, 1-3 disulfoimidazolium trifluoroacetate [BDSIM][TFA]	Brown viscous liquid; FT-IR (KBr) υ cm^{-1}: 3438,3154, 3012, 2969, 2929, 2865, 2729,1751, 1629, 1500, 1462, 1191, 1049, 876, 850, 760, 680, 580 and 451;^{1}H NMR (400MHz, DMSO-d_6) : δ 12.89 (s, 2H), 7.41 (s, 2H), 2.83 (t, J =8.0Hz, 2H), 1.62-1.55 (m, 2H), 1.19-1.13 (m, 2H), 0.76 (t, J= 8.Hz, 3H) ; ^{13}C NMR (100 MHz, DMSO-d_6): δ 158.6, 147.8, 119.1, 29.1, 25.0, 21.6 and 13.6; CHN analysis(%) :Cal. C 26.93, H 4.02, N 6.98; Found C 26.81, H 4.04, N 6.90.

3.4.3 NMR spectra of the [EDSIM][TFA] & [BDSIM][TFA] ionic liquids

1. ^{1}H NMR spectra of [EDSIM][TFA]
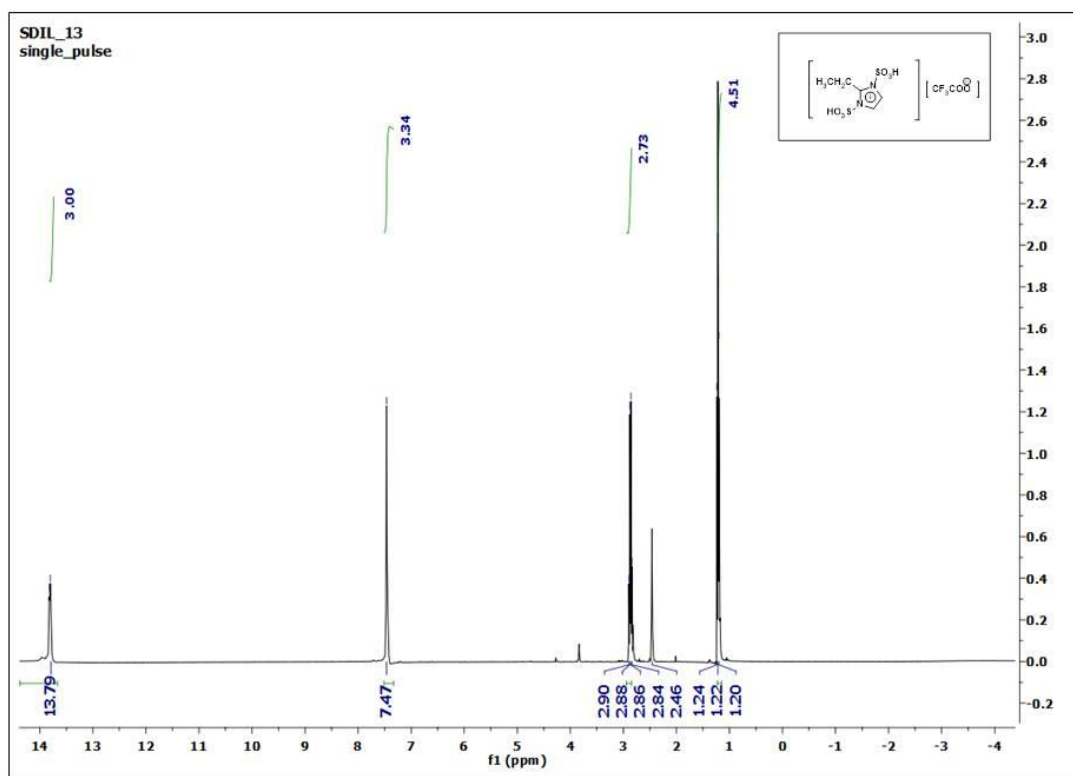
2. ^{13}C NMR spectra of [EDSIM][TFA]
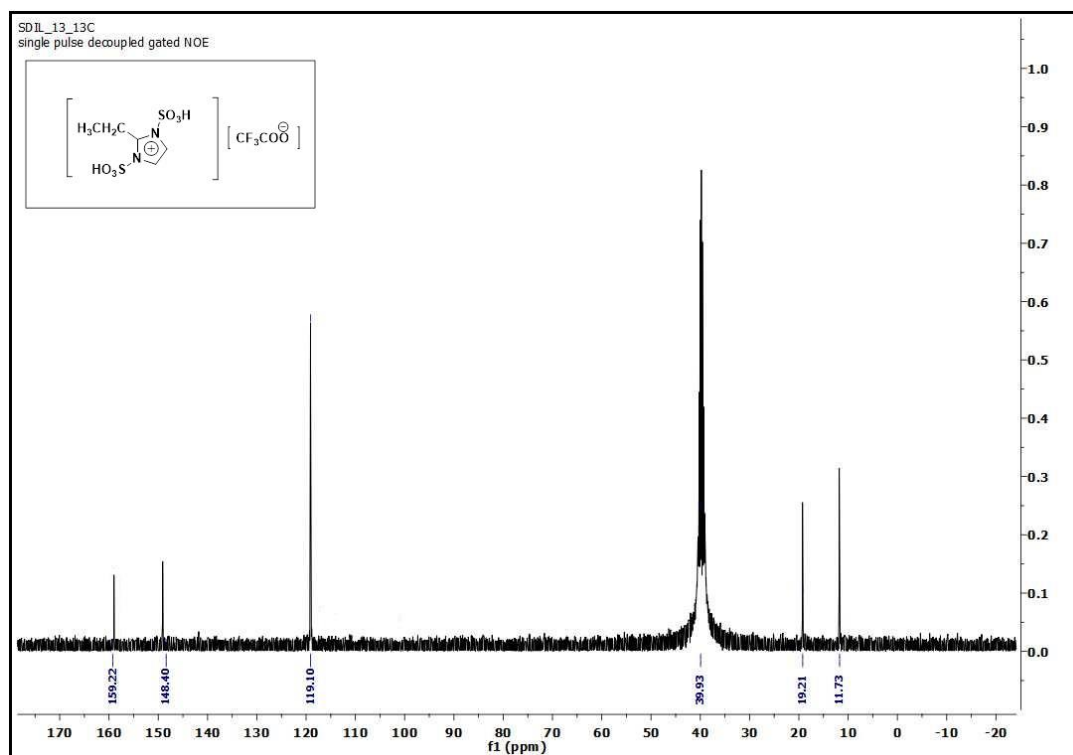
3. ^{1}H NMR spectra of [BDSIM][TFA]
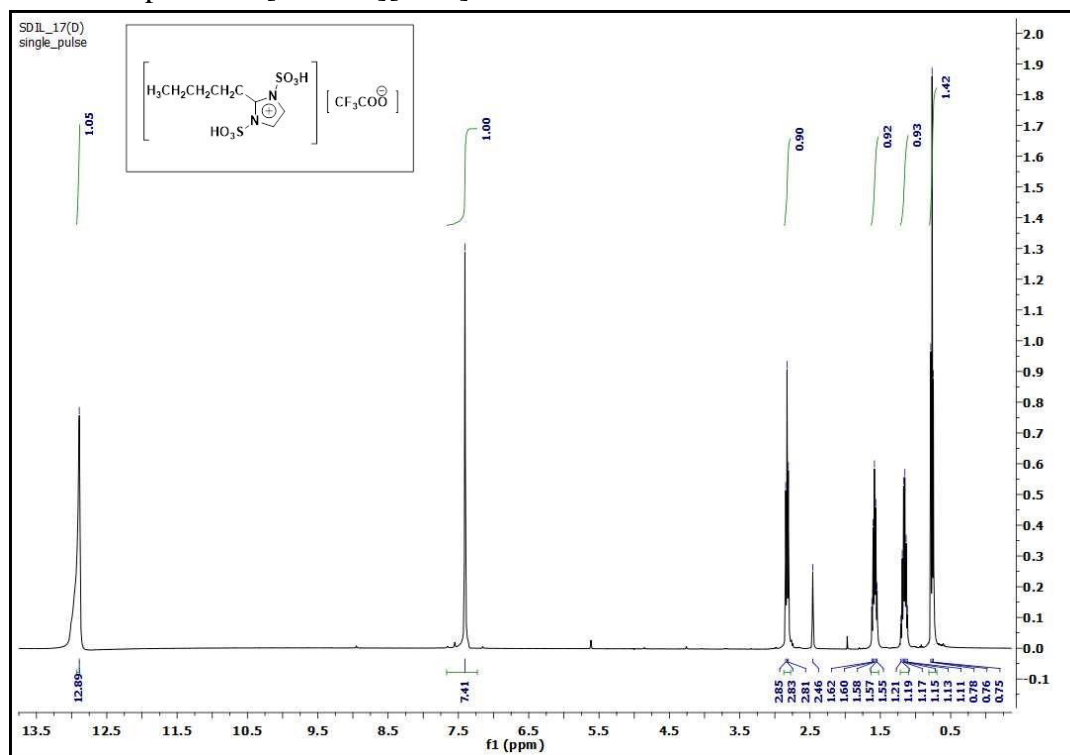
4. ^{13}C NMR of [BDSIM][TFA]
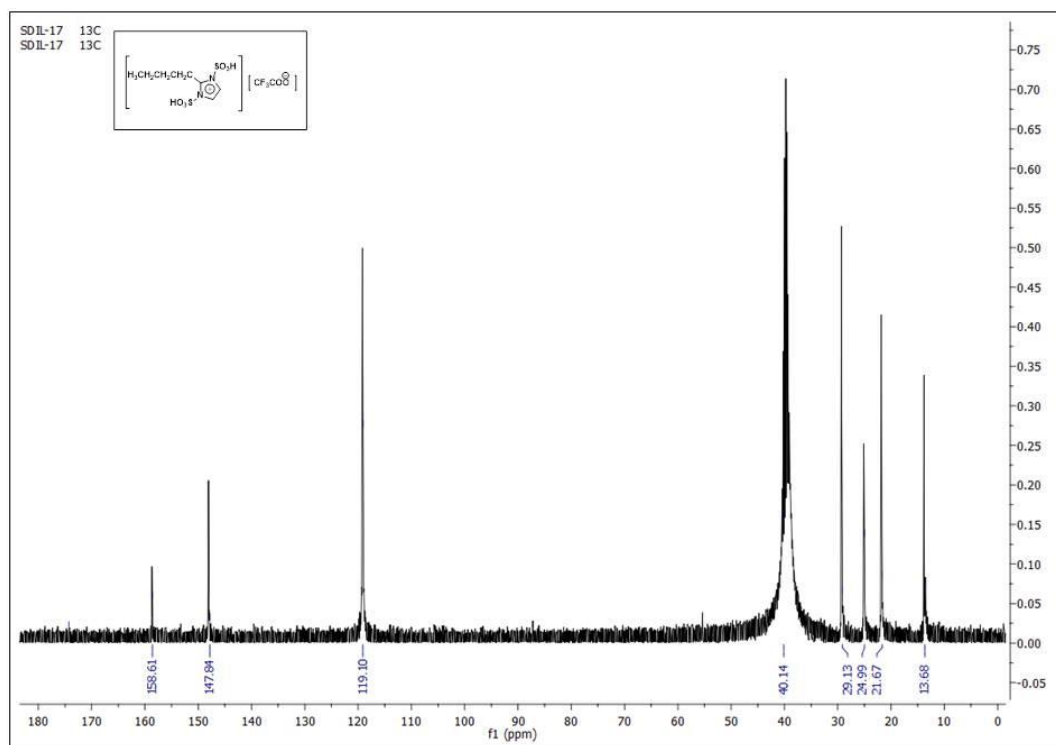
Bibliography

[1]   Dutta, A. K., Gogoi, P., and Borah, R. Synthesis of dibenzoxanthene and acridine derivatives catalyzed by 1,3-disulfonic acid imidazolium carboxylate ionic liquids. *RSC Advances*, 4:41287-41291, 2014.

[2]   Vafaeezadeh, M. and Alinezhad, H. Brønsted acidic ionic liquids: Green catalysts for essential organic reactions. *Journal of Molecular Liquids*, 218:95-105, 2016.

[3]   Watanabe, M., Thomas, M. L., Zhang, S., Ueno, K., Yasuda, T., and Dokko, K. Application of ionic liquids to energy storage and conversion materials and devices. *Chemical Reviews*, 117:7190-7239, 2017.

[4]   Xu, F., Sun, J., Konda, N. M., Shi, J., Dutta, T., Scown, C. D., Simmons, B. A., and Singh, S. Transforming biomass conversion with ionic liquids: process intensification and the development of a high-gravity, one-pot process for the production of cellulosic ethanol. *Energy & Environmental Science*, 9:1042-1049, 2016..

[5]   da Costa Lopes, A. M. and Bogel-Łukasik, R. Acidic ionic liquids as sustainable approach of cellulose and lignocellulosic biomass conversion without additional catalysts. *ChemSusChem*, 8:947-965, 2015.

[6]   Lu, J., Yan, F., and Texter, J. Advanced applications of ionic liquids in polymer science. *Progress in Polymer Science*, 34:431-448, 2009.

[7]   Shikha, P. and Kang, T. S. Facile and green one pot synthesis of zinc sulphide quantum dots employing zinc-based ionic liquids and their photocatalytic activity. *New Journal of Chemistry*, 41:7407-7416, 2017.

[8]   Leu, M., Campbell, P., and Mudring, A. V. Synthesis of luminescent semiconductor nanoparticles in ionic liquids–the importance of the ionic liquid in the formation of quantum dots. *Green Chemistry Letters and Reviews*, 14:128-136, 2021.

[9]   Ho, T. D., Zhang, C., Hantao, L. W., and Anderson, J. L. Ionic liquids in analytical chemistry: fundamentals, advances, and perspectives. *Analytical Chemistry*, 86:262-285, 2014.

[10] Aleixandre, M. and Nakamoto, T. Study of room temperature ionic liquids as gas sensing materials in quartz crystal microbalances. *Sensors*, 20:4026, 2020.

[11] Nagarajan, S. and Kandasamy, E. Reusable 1, 2, 4-triazolium based brønsted acidic room temperature ionic liquids as catalyst for Mannich base reaction. *Catalysis Letters*, *144*:1507-1514, 2014.

[12] Heravi, M. M., Hashemi, E., Beheshtiha, Y. S., Kamjou, K., Toolabi, M., and Hosseintash, N. Solvent-free multicomponent reactions using the novel N-sulfonic acid modified poly (styrene-maleic anhydride) as a solid acid catalyst. *Journal of Molecular Catalysis A: Chemical*, 392:173-180, 2014.

[13] Hajipour, A. R., Ghayeb, Y., Sheikhan, N., and Ruoho, A. E. Brønsted acidic ionic liquid as an efficient and reusable catalyst for one-pot synthesis of 1-amidoalkyl 2-naphthols under solvent-free conditions. *Tetrahedron Letters*, 50:5649-5651, 2009.

[14] Fei, Z., Geldbach, T. J., Zhao, D., and Dyson, P. J. From dysfunction to bis-function: on the design and applications of functionalised ionic liquids. *Chemistry– A European Journal*, 12:2122-2130, 2006.

[15] Fehrmann, R., Riisager, A., and Haumann, M. eds. *Supported ionic liquids: fundamentals and applications*. John Wiley & Sons, pages 1-10. 2014.

[16] Van Doorslaer, C., Wahlen, J., Mertens, P., Binnemans, K., and De Vos, D. Immobilization of molecular catalysts in supported ionic liquid phases. *Dalton Transactions*, 39:8377-8390, 2010.

[17] Olivier-Bourbigou, H., Magna, L., and Morvan, D. Ionic liquids and catalysis: Recent progress from knowledge to applications. *Applied Catalysis A: General*, 373:1-56, 2010.

[18] Hajipour, A. R. and Rafiee, F. Acidic Brønsted ionic liquids. *Organic Preparations and Procedures International*, 42:285-362, 2010.

[19] Chiappe, C. and Rajamani, S. Structural effects on the physico-chemical and catalytic properties of acidic ionic liquids: an overview. *European Journal of Organic Chemistry*, 2011:5517-5539, 2011.

[20] Dorbritz, S., Ruth, W., and Kragl, U. Investigation on aggregate formation of ionic liquids. *Advanced Synthesis & Catalysis*, 347:1273-1279, 2005.

[21] Boruń, A., Fernandez, C., and Bald, A. Conductance studies of aqueous ionic liquids solutions [emim][BF_4] and [bmim][BF_4] at temperatures from (283.15 to 318.15) K. *International Journal of Electrochemical Science*, 10:2120-2129, 2015.

[22] Zolfigol, M. A., Khazaei, A., Moosavi-Zare, A. R., Zare, A., and Khakyzadeh, V. Rapid synthesis of 1-amidoalkyl-2-naphthols over sulfonic acid functionalized imidazolium salts. *Applied Catalysis A: General*, 400:70-81, 2011.

[23] Zolfigol, M. A., Khazaei, A., Moosavi-Zare, A. R., and Zare, A. Ionic liquid 3-methyl-1-sulfonic acid imidazolium chloride as a novel and highly efficient catalyst for the very rapid synthesis of bis (indolyl) methanes under solvent-free conditions. *Organic Preparations and Procedures International*, 42:95-102, 2010.

[24] Zolfigol, M. A., Khazaei, A., Moosavi-Zare, A. R., and Zare, A. 3-Methyl-1-Sulfonic acid imidazolium chloride as a new, efficient and recyclable catalyst and solvent for the preparation of N-sulfonyl imines at room temperature. *Journal of the Iranian Chemical Society*, 7:646-651, 2010.

[25] Akbari, J., Heydari, A., Reza Kalhor, H., and Kohan, S. A. Sulfonic acid functionalized ionic liquid in combinatorial approach, a recyclable and water tolerant-acidic catalyst for one-pot Friedlander quinoline synthesis. *Journal of Combinatorial Chemistry*, 12:137-140, 2010.

[26] Kore, R. and Srivastava, R. Influence of–SO3H functionalization (N-SO$_3$H or NR-SO$_3$H, where R= alkyl/benzyl) on the activity of Brönsted acidic ionic liquids in the hydration reaction. *Tetrahedron Letters*, 53(26):3245-3249, 2012.

[27] Gogoi, P., Dutta, A. K., Sarma, P., and Borah, R. Development of Brönsted–Lewis acidic solid catalytic system of 3-methyl-1-sulfonic acid imidazolium transition metal chlorides for the preparation of bis (indolyl) methanes. *Applied Catalysis A: General*, 492:133-139, 2015.

[28] Dutta, A. K., Gogoi, P., Saikia, S., and Borah, R. N, N-disulfo-1,1,3,3-tetramethylguanidinium carboxylate ionic liquids as reusable homogeneous catalysts for multicomponent synthesis of tetrahydrobenzo [a] xanthene and tetrahydrobenzo [a] acridine derivatives. *Journal of Molecular Liquids*, *225*:585-591, 2017.

[29] Dutta, A. K., Gogoi, P., and Borah, R. Triphenylsulfophosphonium chlorometallates as efficient heterogeneous catalysts for the three-component synthesis of 2,3-dihydro-1,2,3-trisubstituted-1H-naphth[*1,2-e*][*1,3*]oxazines. *Polyhedron*, 123:184-191, 2017.

[30] Moosavi-Zare, A. R., Zolfigol, M. A., Zarei, M., Zare, A., and Khakyzadeh, V. Preparation, characterization and application of ionic liquid sulfonic acid

functionalized pyridinium chloride as an efficient catalyst for the solvent-free synthesis of 12-aryl-8,9,10,12-tetrahydrobenzo [a]-xanthen-11-ones. *Journal of Molecular Liquids*, 186:63-69, 2013.

[31] Sarma, P., Dutta, A. K., and Borah, R. Design and Exploration of–SO₃H Group Functionalized Brønsted Acidic Ionic Liquids (BAILs) as Task-Specific Catalytic Systems for Organic Reactions: A Review of Literature. *Catalysis Surveys from Asia*, 21:70-93, 2017.

[32] Thawarkar, S., Khupse, N. D., and Kumar, A. Comparative investigation of the ionicity of aprotic and protic ionic liquids in molecular solvents by using conductometry and NMR spectroscopy. *ChemPhysChem*, 17:1006-1017, 2016.

[33] Wu, T. Y., Su, S. G., Lin, Y. C., Wang, H. P., Lin, M. W., Gung, S. T., and Sun, I. W. Electrochemical and physicochemical properties of cyclic amine-based Brønsted acidic ionic liquids. *Electrochimica Acta*, 56:853-862, 2010.

[34] Khodadadi-Moghaddam, M., Habibi-Yangjeh, A., and Gholami, M.R. Solvatochromic parameters for binary mixtures of an ionic liquid with various protic molecular solvents. *Monatshefte für Chemie-Chemical Monthly*, 140:329-334, 2009.

[35] Buzzeo, M. C., Hardacre, C., and Compton, R. G. Extended electrochemical windows made accessible by room temperature ionic liquid/organic solvent electrolyte systems. *ChemPhysChem*, 7:176-180, 2006.

[36] Boruń, A. and Bald, A. Ionic association and conductance of ionic liquids in dichloromethane at temperatures from 278.15 to 303.15 K. *Ionics*, 22:859-867, 2016.

[37] De Vos, N., Maton, C., and Stevens, C. V. Electrochemical stability of ionic liquids: general influences and degradation mechanisms. *ChemElectroChem*, 1:1258-1270, 2014.

[38] Seki, S., Kobayashi, T., Kobayashi, Y., Takei, K., Miyashiro, H., Hayamizu, K., Tsuzuki, S., Mitsugi, T., and Umebayashi, Y. Effects of cation and anion on physical properties of room-temperature ionic liquids. *Journal of Molecular Liquids*, 152:9-13, 2010.

[39] Thawarkar, S., Khupse, N. D., and Kumar, A. Solvent-mediated molar conductivity of protic ionic liquids. *Physical Chemistry Chemical Physics*, 17:475-482, 2015.

[40] Pereiro, A. B., Araújo, J. M., Oliveira, F. S., Bernardes, C. E., Esperança, J. M., Lopes, J. N. C., Marrucho, I. M., and Rebelo, L. P. Inorganic salts in purely ionic liquid media: the development of high ionicity ionic liquids (HIILs). *Chemical Communications*, 48:3656-3658, 2012.

[41] Rupp, A., Roznyatovskaya, N., Scherer, H., Beichel, W., Klose, P., Sturm, C., Hoffmann, A., Tübke, J., Koslowski, T., and Krossing, I. Size matters! On the way to ionic liquid systems without ion pairing. *Chemistry–A European Journal*, 20:9794-9804, 2014.

[42] Bešter-Rogač, M., Stoppa, A., Hunger, J., Hefter, G., and Buchner, R. Association of ionic liquids in solution: a combined dielectric and conductivity study of [bmim][Cl] in water and in acetonitrile. *Physical Chemistry Chemical Physics*, 13:17588-17598, 2011.

[43] O'Mahony, A. M., Silvester, D. S., Aldous, L., Hardacre, C., and Compton, R.G. Effect of water on the electrochemical window and potential limits of room-temperature ionic liquids. *Journal of Chemical & Engineering Data*, 53:2884-2891, 2008.

[44] Zhou, H., Chen, L., Wei, Z., Lu, Y., Peng, C., Zhang, B., Zhao, X., Wu, L., and Wang, Y. Effect of ionic composition on physicochemical properties of mono-ether functional ionic liquids. *Molecules*, 24:3112, 2019.

[45] Takamuku, T., Kyoshoin, Y., Shimomura, T., Kittaka, S., and Yamaguchi, T. Effect of water on structure of hydrophilic imidazolium-based ionic liquid. *The Journal of Physical Chemistry B*, 113:10817-10824, 2009.

[46] Handy, S. T. and Okello, M. The 2-position of imidazolium ionic liquids: Substitution and exchange. *The Journal of organic chemistry*, 70:1915-1918, 2005.

[47] Xu, L., Cui, X., Zhang, Y., Feng, T., Lin, R., Li, X., and Jie, H. Measurement and correlation of electrical conductivity of ionic liquid [EMIM][DCA] in propylene carbonate and γ-butyrolactone. *Electrochimica Acta*, 174:900-907, 2015.

[48] Boruń, A. and Bald, A. Ionic association and conductance of ionic liquids in dichloromethane at temperatures from 278.15 to 303.15 K. *Ionics*, 22:859-867, 2016.

[49] Amarasekara, A. S. Acidic ionic liquids. *Chemical reviews*, 116:6133-6183, 2016.